



# Differential Expression of Genes Regulating Store-operated Calcium Entry in Conjunction With Mitochondrial Dynamics as Potential Biomarkers for Cancer: A Single-Cell RNA Analysis

## OPEN ACCESS

### Edited by:

Rajkumar S Kalra,  
Okinawa Institute of Science and  
Technology Graduate University,  
Japan

### Reviewed by:

Jeremy Smyth,  
Uniformed Services University of the  
Health Sciences, United States  
Prashanth Thevkar Nagesh,  
Harvard Medical School,  
United States

### \*Correspondence:

Ajaikumar B. Kunnumakkara  
kunnumakkara@iitg.ac.in  
ajai78@gmail.com

### Specialty section:

This article was submitted to  
Human and Medical Genomics,  
a section of the journal  
Frontiers in Genetics

**Received:** 31 January 2022

**Accepted:** 27 April 2022

**Published:** 31 May 2022

### Citation:

Hegde M, Daimary UD, Jose S,  
Sajeev A, Chinnathambi A, Alharbi SA,  
Shakibaei M and Kunnumakkara AB  
(2022) Differential Expression of Genes  
Regulating Store-operated Calcium  
Entry in Conjunction With  
Mitochondrial Dynamics as Potential  
Biomarkers for Cancer: A Single-Cell  
RNA Analysis.  
Front. Genet. 13:866473.  
doi: 10.3389/fgene.2022.866473

Mangala Hegde<sup>1,2</sup>, Uzini Devi Daimary<sup>1,2</sup>, Sandra Jose<sup>1,2</sup>, Anjana Sajeev<sup>1,2</sup>,  
Arunachalam Chinnathambi<sup>3</sup>, Sulaiman Ali Alharbi<sup>3</sup>, Mehdi Shakibaei<sup>4</sup> and  
Ajaikumar B. Kunnumakkara<sup>1,2\*</sup>

<sup>1</sup>Cancer Biology Laboratory, Department of Biosciences and Bioengineering, Indian Institute of Technology-Guwahati, Guwahati, India, <sup>2</sup>DBT-AIST International Center for Translational and Environmental Research, Indian Institute of Technology-Guwahati, Guwahati, India, <sup>3</sup>Department of Botany and Microbiology, College of Science, King Saud University, Riyadh, Saudi Arabia, <sup>4</sup>Musculoskeletal Research Group and Tumor Biology, Faculty of Medicine, Institute of Anatomy, Ludwig-Maximilian-University Munich, Munich, Germany

Regulation of intracellular concentration of calcium levels is crucial for cell signaling, homeostasis, and in the pathology of diseases including cancer. Agonist-induced entry of calcium ions into the non-excitatory cells is mediated by store-operated calcium channels (SOCs). This pathway is activated by the release of calcium ions from the endoplasmic reticulum and further regulated by the calcium uptake through mitochondria leading to calcium-dependent inactivation of calcium-release activated calcium channels (CARC). SOCs including stromal interaction molecules (STIM) and ORAI proteins have been implicated in tumor growth, progression, and metastasis. In the present study, we analyzed the mRNA and protein expression of genes mediating SOCs—STIM1, STIM2, ORAI1, ORAI2, ORAI3, TRPC1, TRPC3, TRPC4, TRPC5, TRPC6, TRPC7, TRPV1, TRPV2, TRPM1, and TRPM7 in head and neck squamous cell cancer (HNSC) patients using TCGA and CPTAC analysis. Further, our *in silico* analysis showed a significant correlation between the expression of SOCs and genes involved in the mitochondrial dynamics (MDGs) both at mRNA and protein levels. Protein-protein docking results showed lower binding energy for SOCs with MDGs. Subsequently, we validated these results using gene expression and single-cell RNA sequencing datasets retrieved from Gene Expression Omnibus (GEO). Single-cell gene expression analysis of HNSC tumor tissues revealed that SOCs expression is remarkably associated with the MDGs expression in both cancer and fibroblast cells.

**Keywords:** head and neck cancer, store-operated calcium channels, mitochondrial dynamics, TCGA database, CPTAC database, gene expression omnibus

## INTRODUCTION

Calcium ( $\text{Ca}^{2+}$ ) is a ubiquitous intracellular second messenger that controls a wide range of physiological and pathological processes (Berridge et al., 2003). In metazoans including humans, the store-operated calcium channel entry (SOCE) is the predominant calcium entry mechanism in non-excitatory cells (Parekh and Putney, 2005). The concept of SOCE was first described by James Putney in 1986; however, the molecular signatures and functional validation of SOCE were identified more recently (Putney, 1986). SOCs are activated when  $\text{Ca}^{2+}$  is released from the endoplasmic reticulum, which is necessary for cells to replenish  $\text{Ca}^{2+}$  after signaling processes (Parekh and Putney, 2005). SOCE is implicated in a wide range of biological processes such as transcriptional regulation of gene expression, exocytosis, cellular metabolism, and cell motility (Lewis, 2007; Parekh and Putney, 2005). Among the SOCs, STIM1, and ORAI1 have been shown to be widely expressed. Additionally, closely associated channel subfamilies like transient receptor potential channels (TRPC), TRPV (vanilloid), and TRPM (melastatin) have also been shown to be involved in SOCE mediated  $\text{Ca}^{2+}$  influx (Authi, 2007; Ma et al., 2011; Bastián-Eugenio et al., 2019). A plethora of studies showing the involvement of  $\text{Ca}^{2+}$  in various stages of cancer development and progression led Yang et al. (2009) to investigate the role of STIM1 and ORAI1 in breast cancer cell migration, invasion, and metastasis (Yang et al., 2009). In addition, transcriptomic analysis of glioblastoma tumor tissues showed overexpression of STIM1, ORAI1, and TRPC1 (Scrideli et al., 2008; Alptekin et al., 2015). Moreover, Zhang et al. (2013) demonstrated that SOCE mediated influx of  $\text{Ca}^{2+}$  regulated the migration and metastasis of nasopharyngeal carcinoma both *in vitro* and in zebrafish models (Zhang et al., 2013). Further, Jiang et al. (2007) revealed that TRPM7 is necessary for the proliferation and growth of FaDu and SCC25 cells *in vitro* by siRNA-mediated knockdown of TRPM7 (Jiang et al., 2007). SOCs have also been proposed as potential therapeutic targets for various inflammatory disorders and cancer (Feske, 2019; Khan et al., 2020; Chang et al., 2021). Recent studies have shown that non-steroidal anti-inflammatory drugs (NSAIDs) including sulindac, salicylate, flurbiprofen, and indomethacin inhibited SOCEs in colon cancer cells (Hernández-Morales et al., 2017; Villalobos et al., 2019). Furthermore, Gualadani et al. (2019) demonstrated the requisite of SOCE for the anti-cancer effect of cisplatin in non-small cell lung carcinoma (Gualadani et al., 2019). Therefore, these studies suggest that SOCs can be used as cancer diagnostic biomarkers and therapeutic targets.

According to the latest GLOBOCAN report on cancer burden worldwide, the prevalence of head and neck cancer is steadily increasing (Sung et al., 2021). Apart from the well-known risk factors such as tobacco, alcohol, and human papillomavirus (HPV), vitamin D insufficiency and defects in calcium signaling have recently been found to play a significant role in the initiation and progression of head and neck cancer (Orell-kotikangas et al., 2012; Singh et al., 2020).

Recently, studies have shown that ORAI1, ORAI2, and STIM1 were significantly elevated in tissues from oral squamous cancer patients compared to normal samples. These studies also reported the significant reduction in proliferation, migration, and invasion upon siRNA-mediated knockdown of ORAI1, ORAI2, and STIM1 in oral

cancer cell lines *in vitro* (Singh et al., 2020; Wang et al., 2022). In the present study, we analyzed the gene and protein expression of SOCs—STIM1, STIM2, ORAI1, ORAI2, ORAI3, TRPC1, TRPC3, TRPC4, TRPC5, TRPC6, TRPC7, TRPV1, TRPV2, TRPM1, and TRPM7 in HNSC using The Cancer Genome Atlas (TCGA) and Clinical Proteomic Tumor Analysis Consortium (CPTAC) analysis. In addition, mitochondrial regulation of calcium ions has shown to play an important role in SOCs mediated calcium entry, and tumor cell mitochondrial dysfunction is proposed to be responsible for SOCs upregulation (Villalobos et al., 2018). Hence, we further analyzed the genes involved in mitochondrial dynamics (MDGs) and found a significant correlation between the expression of SOCs and MDGs both at mRNA and protein levels. Further, docking results showed lower binding energy for SOCs with MDGs. Subsequently, the validation of these results was carried out using datasets downloaded from gene expression omnibus (GEO). Interestingly, single-cell RNA sequence analysis revealed that gene expression of SOCs is remarkably associated with the MDGs in both cancer and fibroblast cells.

## MATERIALS AND METHODS

The methodology of the overall study have been represented in the form of graphical abstract (**Supplementary Figure 1**).

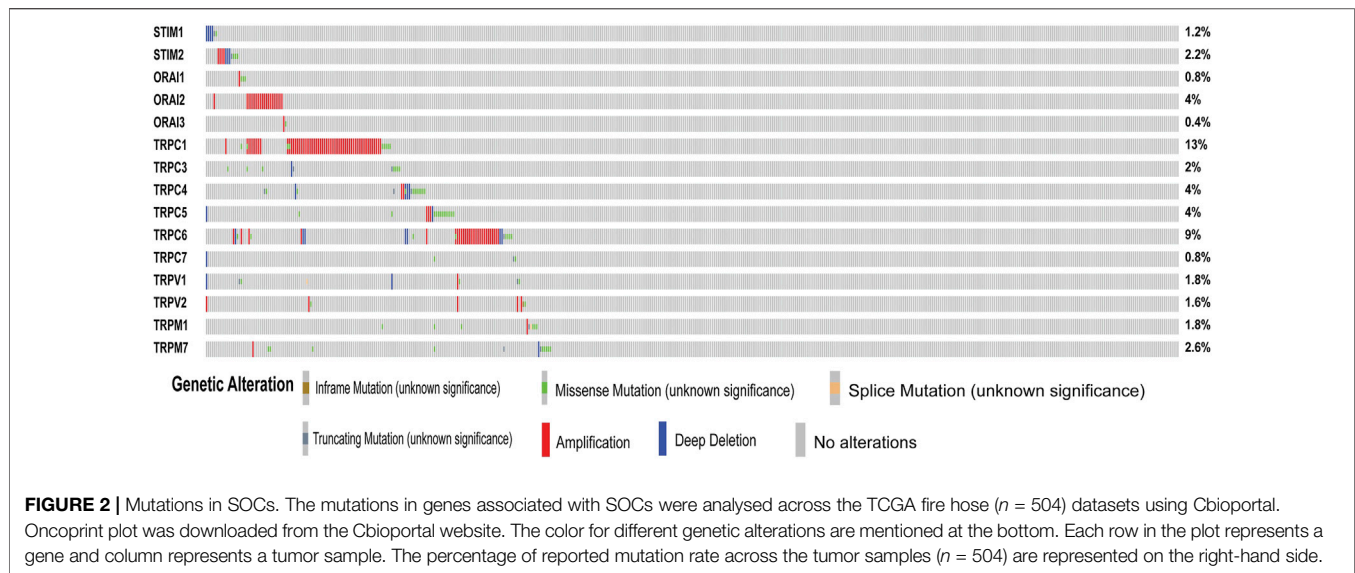
### Gene Ontology Analysis

As a preliminary analysis to show the role of SOCs in signaling pathways we conducted functional enrichment analysis (FEA) to annotate gene ontology (GO) including biological processes (BP), cellular components (CC), molecular function (MF), and pathway enrichment analysis using the Kyoto Encyclopedia of Genes and Genomics (KEGG: <http://www.genome.jp>) (Kanehisa and Goto, 2000). The MF which showed the highest score for SOCs was visualized using gProfiler (Raudvere et al., 2019). The molecular function with significant *p* adj values are shown. These functions are assigned based on either the experiment or Sequence Model (ISM) or Sequence Alignment (ISA) or Sequence Orthology (ISO) or Sequence or structural similarity (ISS) or Genomic context (IGC) or Biological aspect of ancestor (IBA) or Rapid divergence (IRD) or Reviewed computational analysis (RCA) or Electronic annotation (IEA). The disease ontology analysis was conducted to understand the involvement of SOCs in various cancers. The analysis and visualization for disease ontology were performed using the clusterProfiler package developed by Bioconductor for R statistical environment (Yu et al., 2012; Wu et al., 2022). The adjusted *p*-value of less than 0.05 are considered to be significant.

### The Cancer Genome Atlas (TCGA) Analysis

In the next step, we carried out the TCGA analysis to understand the clinical relevance of SOCs in head and neck cancers. The HiSeqV2 TCGA level 3 gene expression data was downloaded using TCGA biolinks version 2.15.1 developed for R statistical environment (Mounir et al., 2019). The data contained 546 tumor samples and 44 normal samples. Correlation analysis was conducted using Corrplot and ggplot2 packages (Wickham et al., 2016; Wei et al., 2017) and survival analysis was performed using Kaplan-Meier





plotter (<http://kmplot.com>) (Lánczky and Györfy, 2021; Nagy et al., 2021). The significance and hazard ratio are shown. Further, we conducted mutational analysis to determine the genomic plasticity of SOCs in head neck cancers. Mutations in potential genes encoding SOCs across the TCGA fire hose dataset for HNSC ( $n = 504$ ) are represented as oncoprint plot downloaded from <http://cbioportal.org> (Cerami et al., 2012). The row of the plot indicates a gene and column indicates the tumor sample.

## Expression Array Data

To further validate the results, we analysed the various expression datasets. Expression profiling dataset GSE171898 contained a total of 323 samples including 208 OSCC tissues from patients treated at Washington University St. Louis and 115 OSCC tissues from patients treated at Vanderbilt University. Illumina Hiseq 3,000 expression profile array data for these samples are available at <https://www.ncbi.nlm.nih.gov/geo/query/acc.cgi?acc=GSE171898>. The patients were stratified based on the HPV data. The platform used for the GSE17898 expression profiling array was GPL21290 and the spot ID is available at <https://www.ncbi.nlm.nih.gov/geo/query/acc.cgi?acc=GPL21290> (Liu et al., 2020).

Single-cell RNA-Seq analysis of head and neck cancer data (GSE103322) were downloaded from the NCBI GEO (Gene Expression Omnibus) database (<https://www.ncbi.nlm.nih.gov/geo/>). The data consists of an expression profile of 5,902 single cells from 18 patients. The platform used for the GSE103322 expression profiling array was GPL18573 and the spot ID is available at <https://www.ncbi.nlm.nih.gov/geo/query/acc.cgi?acc=GPL18573> (Puram et al., 2017).

## Store-Operated Calcium Channels (SOCs) in Mitochondrial Dynamics

The reorganization of ER and  $Ca^{2+}$  ion transfer have been implicated in the mitochondrial fission and apoptosis of

cancer cells (Yedida et al., 2019). Hence, we next analysed the relevance of SOCs with genes involved in mitochondrial dynamics. The correlation between expression of genes involved in SOCs and genes involved in mitochondrial genes for all HNSC patients, and HPV positive and negative HNSC patients were downloaded using Timer 2.0 (<http://timer.comp-genomics.org/>) (Li et al., 2020). The data was visualized using the heatmap function of Graphpad Prism software version 9.2.1. Subsequently, the SOC protein structures and proteins involved in mitochondrial dynamics were downloaded from the protein data bank (Berman et al., 2000). Protein structures for SOCs—STIM1:PDB ID-6YEL (Rathner et al., 2021); STIM2:PDB ID-2L5Y (Zheng et al., 2011); ORAI1:PDB ID-4EHQ (Liu et al., 2012); TRPC5:PDB ID-6YSN (Wright et al., 2020) and MDGs-DNM1L:PDB ID-3W6N (Kishida and Sugio, 2013); MFN1:PDB ID-5GOF (Cao et al., 2017); MFN2:PDB ID-6JFK (Li et al., 2019); OPA1:PDB ID-6JTG (Yu et al., 2020) and FIS1:PDB ID-1PC2 (Suzuki et al., 2003) were downloaded. The docking was performed using Clust Pro version 2.0 (<https://cluspro.bu.edu/login.php>) (Kozakov et al., 2013; Kozakov et al., 2017; Vajda et al., 2017; Desta et al., 2020) and binding energy was calculated using PRODIGY (<https://wenmr.science.uu.nl/prodigy/>) (Vangone and Bonvin, 2015; Xue et al., 2016; Vangone et al., 2019). Gene regulatory network was analyzed using Geneck (<https://lce.biohpc.swmed.edu/geneck/>) (Zhang et al., 2019) and protein-protein interaction network was obtained from string database (<https://string-db.org/>) (Szklarczyk et al., 2019; Szklarczyk et al., 2021).

## Clinical Proteomic Tumor Analysis Consortium (CPTAC) Data Analysis

Since, the protein expression is critical for the signaling pathways and physiological responses, we next analysed

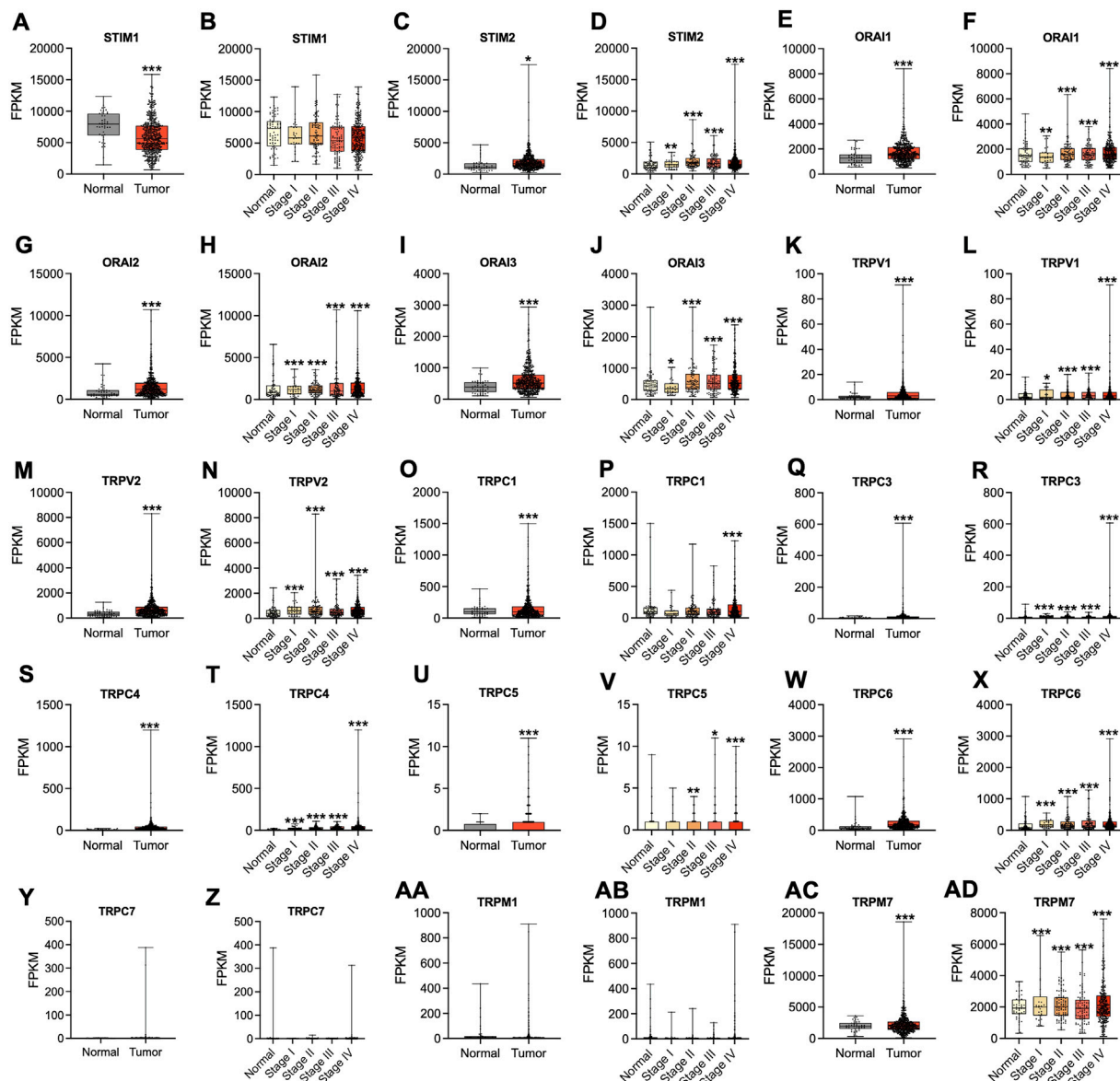


**FIGURE 3 |** Altered mRNA expression of SOC in HNSC. The Hiseq2 gene expression and clinical details of TCGA-HNSC data was downloaded from the TCGA biolinks-Bioconductor package for R statistical environment. The expression levels of SOC (represented as fragments per kilobase per million mapped fragments- FPKM) in normal versus tumor (A,C,E,G,I,K,M,O,Q,S,U,W,Y,AA,AC) and different stages- stage I, stage II, stage III, and stage IV of HNSC (B,D,F,H,J,L,N,P,R,T,V,X,Z,AB,AD) are plotted. The statistical significance is represented as \* $p < 0.05$ , \*\* $p < 0.01$ , \*\*\* $p < 0.0001$ .

the proteomic and phosphoproteomic levels of SOC in HNSC. The CPTAC data for proteomics and phosphoproteomics with clinical data for HNSC was downloaded using Python version 3.0 (Huang et al., 2021). The bar plots were plotted using Graphpad Prism version 9.2.1.

## Histology Analysis

The histopathology images for SOC for HNSC were obtained from Human Protein atlas (<https://www.proteinatlas.org/>) (Uhlén et al., 2015) that is not active.

## Correlation Analysis

The correlation analysis for SOC and MDG gene expression and protein expression were performed using Corplot package for the R programming (Wei et al., 2017).

## Statistical Analysis

Correlation between different parameters was calculated by Pearson correlation analysis. Differences between the groups were evaluated using nonparametric t-test.  $p$ -value  $< 0.05$  was considered to be significant for all the TCGA, CPTAC, and GEO datasets analysis. Statistical analysis was performed using R programming version 3.6.1.

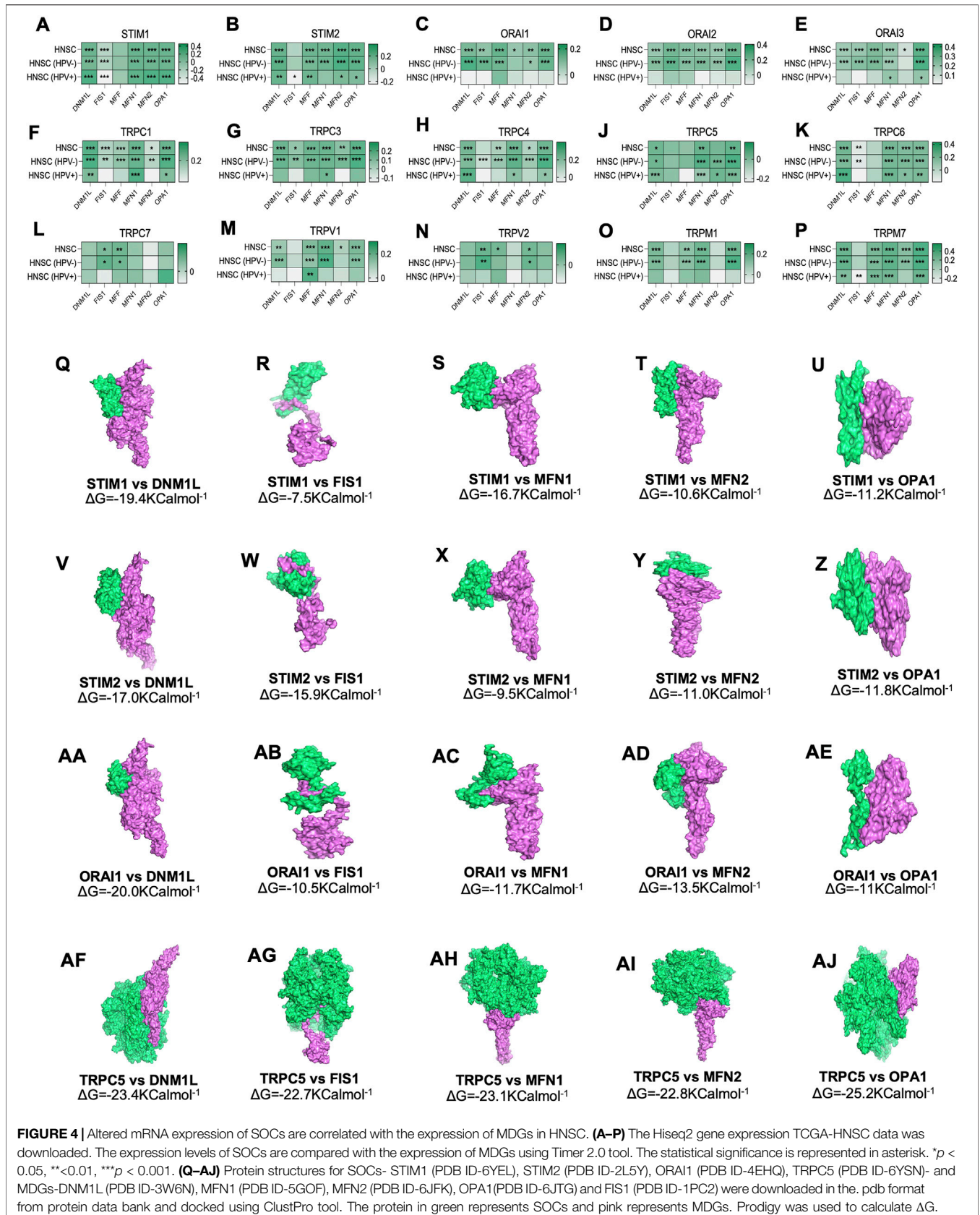
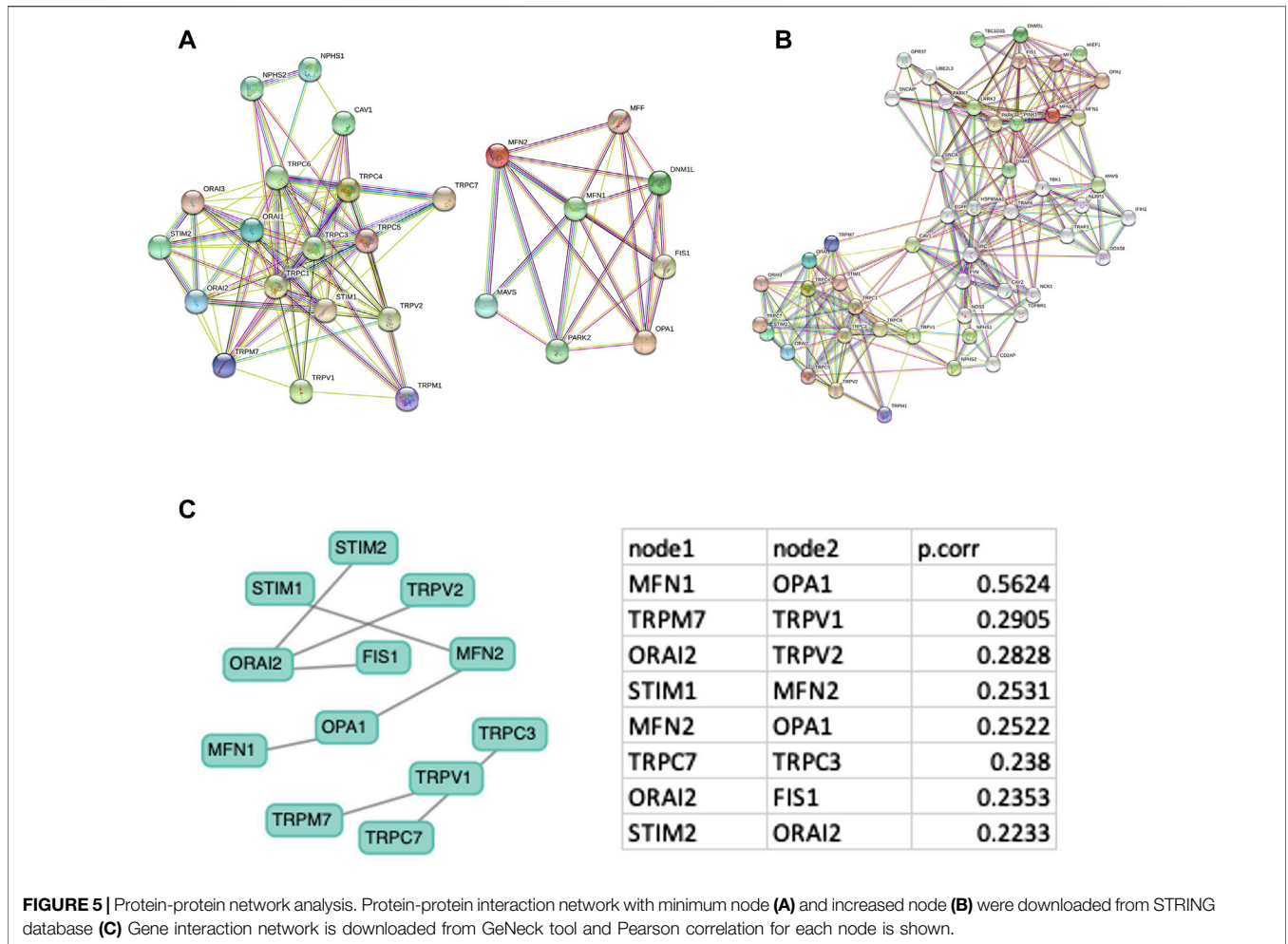


**FIGURE 4 |** Altered mRNA expression of SOC are correlated with the expression of MDGs in HNSC. **(A–P)** The Hiseq2 gene expression TCGA-HNSC data was downloaded. The expression levels of SOC are compared with the expression of MDGs using Timer 2.0 tool. The statistical significance is represented in asterisk. \* $p < 0.05$ , \*\* $< 0.01$ , \*\*\* $p < 0.001$ . **(Q–AJ)** Protein structures for SOC- STIM1 (PDB ID-6YEL), STIM2 (PDB ID-2L5Y), ORAI1 (PDB ID-4EHQ), TRPC5 (PDB ID-6YSN)- and MDGs-DNM1L (PDB ID-3W6N), MFN1 (PDB ID-5GOF), MFN2 (PDB ID-6JFK), OPA1(PDB ID-6JTG) and FIS1 (PDB ID-1PC2) were downloaded in the. pdb format from protein data bank and docked using ClustPro tool. The protein in green represents SOC and pink represents MDGs. Prodigy was used to calculate  $\Delta G$ .



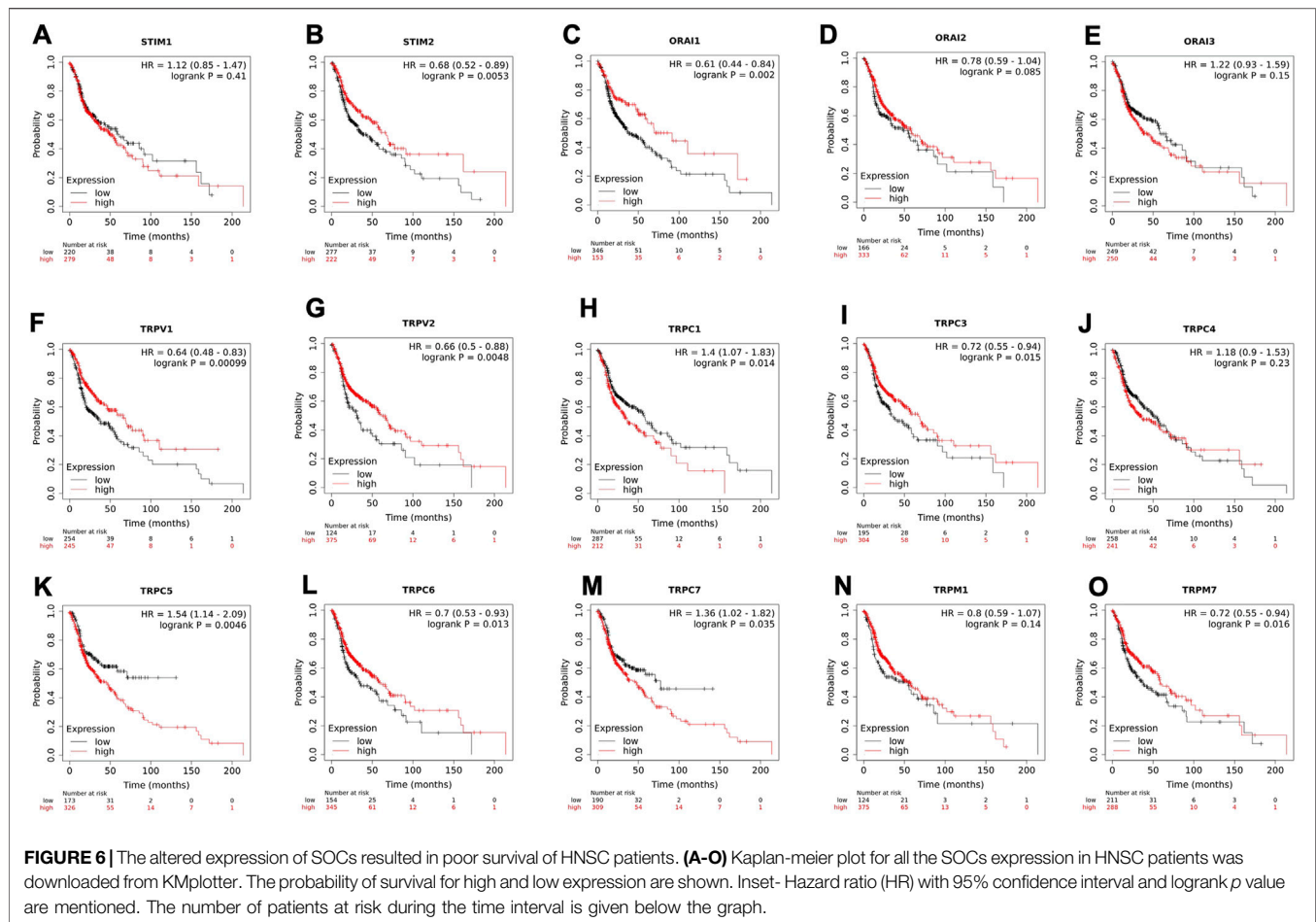
## RESULTS

In the present study, we analyzed the expression of SOC mRNA, proteins, and phosphoproteins of HNSC by *in silico* approaches. In addition, we have also shown the mutations in these genes to understand the effect of genetic alterations on their expression in HNSC patients. Next, we cohered the gene and protein expression levels of SOC versus MDGs and correlated their expression with the survival risk of HNSC patients. Further, we performed docking to understand the binding efficiency of SOCE proteins with MDGs. To our knowledge, this is the first comprehensive study that links the SOC gene expression to MDGs and potential risk of early death in HNSC.

### Differential Expression of Store-Operated Calcium Channel Entry in Head and Neck Squamous Cell Cancer

In the first step, GO and KEGG pathway analysis was carried out for fifteen SOC genes- STIM1, STIM2, ORAI1, ORAI2, ORAI3, TRPC1, TRPC3, TRPC4, TRPC5, TRPC6, TRPC7, TRPV1,

TRPV2, TRPM1, and TRPM7 using clusterProfiler to understand their function in MF, CC, and BP. The genes were enriched mainly for MF (**Figure 1A**). The molecular function enrichment using gProfiler identified SOC genes involvement in inositol binding activity and ATPase binding activity which are crucial for cell signaling and regulation of cellular functions apart from the usual calcium transporter, ion transporter, and transmembrane transporter activities of SOC (**Figure 1B**). The disease enrichment analysis using ClusterProfiler showed that these genes are involved in pulmonary hypertension, disorders related to muscles, lymphoproliferative disorders, malignant eye tumors, cerebellar medulloblastoma, immune system diseases, and inflammatory disorders (**Figure 1C**). This indicated that SOC play critical role in tumor development and progression. Further, we analysed for the mutation in SOC across TCGA fire hose datasets containing 504 samples for HNSC. The mutation analysis showed 1.2% mutation in STIM1 (6/504), 2.2% mutation in STIM2 (11/504), 0.8% mutation in ORAI1 (4/504), 4% mutation in ORAI2 (20/504), 0.4% mutation in ORAI3 (2/504), 13% in TRPC1 (64/504), 2% mutation in TRPC3 (10/504), 4% mutation in TRPC4 (20/504),



4% mutation in TRPC5 (20/504), 9% mutation in TRPC6 (43/504), 0.8% mutation in TRPC7 (4/504), 1.8% mutation in TRPV1 (9/504), 1.6% mutation in TRPV2 (8/504), 1.8% mutation in TRPM1 (9/504), and 2.6% mutation in TRPM7 (13/504). This low percentage of mutations indicated that mutation is solely not responsible for the aberration in the SOCs expression (Figure 2). Hence, we further analysed the mRNA expression of SOCs. The mRNA expression of SOCs genes across TCGA-HNSC data was downloaded from the TCGA biolinks R package. The data showed significant upregulation of STIM2 ( $p < 0.05$ ), ORAI1 ( $p < 0.001$ ), ORAI2 ( $p < 0.001$ ), ORAI3 ( $p < 0.001$ ), TRPC1 ( $p < 0.001$ ), TRPC3 ( $p < 0.001$ ), TRPC4 ( $p < 0.001$ ), TRPC5 ( $p < 0.001$ ), TRPC6 ( $p < 0.001$ ), TRPV1 ( $p < 0.001$ ), TRPV2 ( $p < 0.001$ ), and TRPM7 ( $p < 0.001$ ) and downregulation of STIM1 ( $p < 0.001$ ) and TRPM1 ( $p > 0.05$ ) were observed across HNSC samples. The expression level of TRPC7 was found to be low in both controls and HNSC patients and was insignificant. We also conducted the stage-wise expression analysis of these genes in HNSC. The data showed significant upregulation of STIM2 (Normal vs. stage I:  $p < 0.01$ ; Normal vs. stage II:  $p < 0.001$ ; Normal vs. stage III:  $p < 0.001$ ; Normal vs. stage IV:  $p < 0.001$ ), ORAI1 (Normal vs. stage I:  $p < 0.01$ ; Normal vs. stage II:  $p < 0.001$ ; Normal vs. stage III:  $p < 0.001$ ; Normal vs. stage IV:  $p < 0.001$ ),

ORAI2 (Normal vs. stage I:  $p < 0.001$ ; Normal vs. stage II:  $p < 0.001$ ; Normal vs. stage III:  $p < 0.001$ ; Normal vs. stage IV:  $p < 0.001$ ), ORAI3 (Normal vs. stage I:  $p < 0.05$ ; Normal vs. stage II:  $p < 0.001$ ; Normal vs. stage III:  $p < 0.001$ ; Normal vs. stage IV:  $p < 0.001$ ), TRPC3 (Normal vs. stage I:  $p < 0.001$ ; Normal vs. stage II:  $p < 0.001$ ; Normal vs. stage III:  $p < 0.001$ ; Normal vs. stage IV:  $p < 0.001$ ), TRPC4 (Normal vs. stage I:  $p < 0.001$ ; Normal vs. stage II:  $p < 0.001$ ; Normal vs. stage III:  $p < 0.001$ ; Normal vs. stage IV:  $p < 0.001$ ), TRPC5 (Normal vs. stage I:  $p > 0.05$ ; Normal vs. stage II:  $p < 0.01$ ; Normal vs. stage III:  $p > 0.05$ ; Normal vs. stage IV:  $p < 0.001$ ), TRPC6 (Normal vs. stage I:  $p < 0.001$ ; Normal vs. stage II:  $p < 0.001$ ; Normal vs. stage III:  $p < 0.001$ ; Normal vs. stage IV:  $p < 0.001$ ), TRPV1 (Normal vs. stage I:  $p < 0.05$ ; Normal vs. stage II:  $p < 0.001$ ; Normal vs. stage III:  $p < 0.001$ ; Normal vs. stage IV:  $p < 0.001$ ), TRPV2 (Normal vs. stage I:  $p < 0.001$ ; Normal vs. stage II:  $p < 0.001$ ; Normal vs. stage III:  $p < 0.001$ ; Normal vs. stage IV:  $p < 0.001$ ), and TRPM7 (Normal vs. stage I:  $p < 0.001$ ; Normal vs. stage II:  $p < 0.001$ ; Normal vs. stage III:  $p < 0.001$ ; Normal vs. stage IV:  $p < 0.001$ ) across all the stages of HNSC. TRPC1 ( $p < 0.001$ ) level was found to be significantly altered in stage IV disease. STIM1, TRPC7, and TRPM1 were found to be non-significant across the stages of HNSC compared to controls (Figures 3A-D). These results indicated that SOCs are differentially

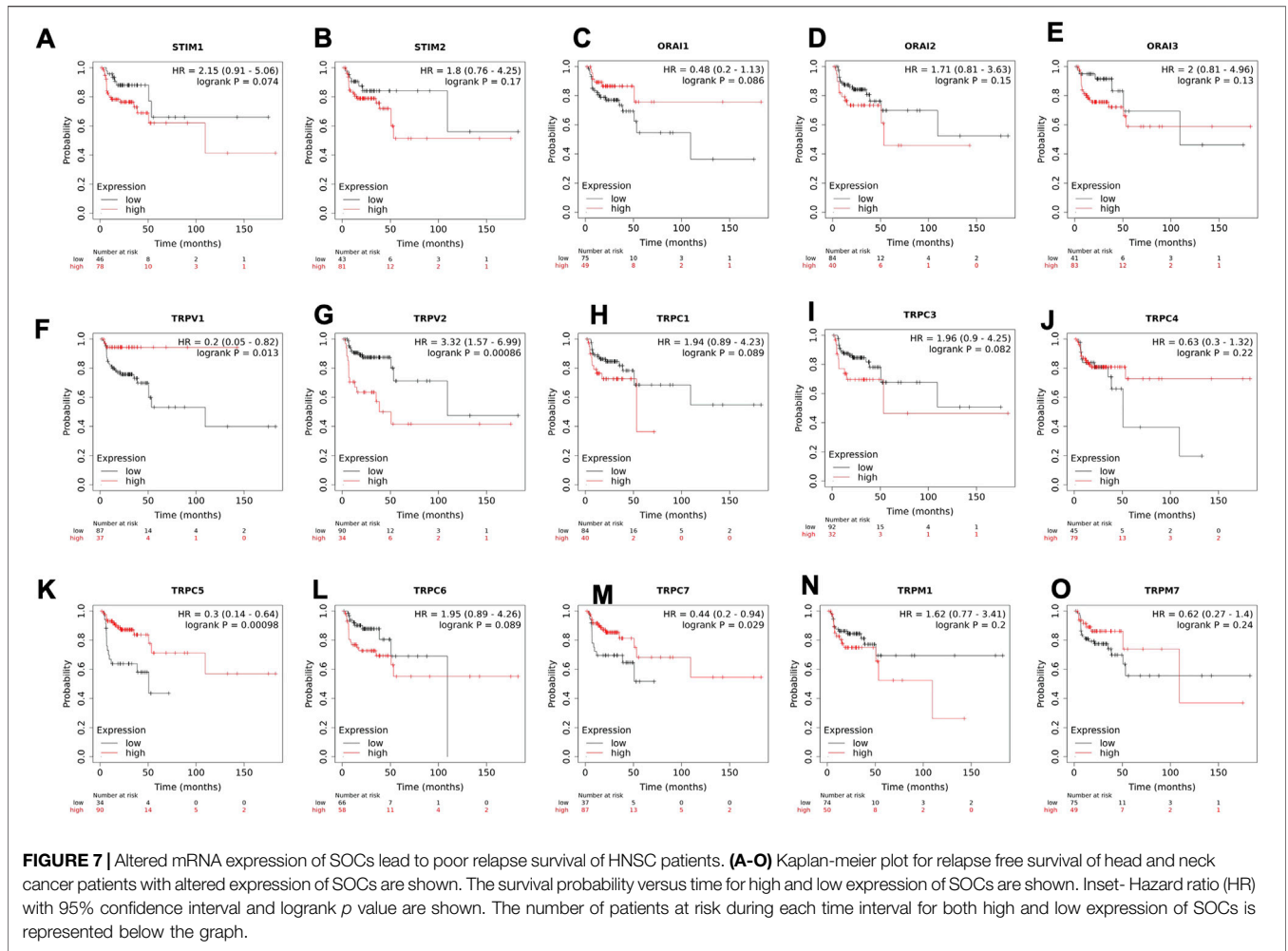


**FIGURE 7 |** Altered mRNA expression of SOC genes lead to poor relapse survival of HNSC patients. (A–O) Kaplan-meier plot for relapse free survival of head and neck cancer patients with altered expression of SOC genes are shown. The survival probability versus time for high and low expression of SOC genes are shown. Inset- Hazard ratio (HR) with 95% confidence interval and logrank *p* value are shown. The number of patients at risk during each time interval for both high and low expression of SOC genes is represented below the graph.

expressed in various stages of head and neck cancers and could be a potential biomarker of HNSC.

### Correlation of Store-Operated Calcium Channels Gene Expression and Genes Involved in Mitochondrial Dynamics (MDGs)

The expression of SOC genes and mitochondrial dynamics regulatory genes- DNMI1L, FIS1, MFF, MFN1, MFN2, OPA1 across TCGA-HNSC data were conducted using Timer 2.0 webtool. The expression of SOC genes was found to be remarkably associated with the expression of DNMI1L, FIS1, MFN1, MFN2, and OPA1. Similarly, expression of SOC genes with MDGs in HPV positive and HPV negative HNSC patient samples are also shown (Figures 4A–P). Next, we downloaded available protein structures for SOC genes (STIM1, STIM2, ORAI1, TRPC5) and mitochondrial fission and fusion regulatory genes (DNMI1L, FIS1, MFF, MFN1, MFN2, and OPA1) from the protein data bank. Protein-protein docking using ClustPro and Prodigy showed high negative binding energy for these proteins—STIM1 vs. DNMI1L:ΔG = -19.4KCalmol<sup>-1</sup>, STIM1

vs. FIS1:ΔG = -7.5KCalmol<sup>-1</sup>, STIM1 vs. MFN1:ΔG = -16.7KCalmol<sup>-1</sup>, STIM1 vs. MFN2:ΔG = -10.6KCalmol<sup>-1</sup>, STIM1 vs. OPA1:ΔG = -11.2KCalmol<sup>-1</sup>; STIM2 vs. DNMI1L:ΔG = -17.0KCalmol<sup>-1</sup>; STIM2 vs. FIS1:ΔG = -15.9KCalmol<sup>-1</sup>, STIM2 vs. MFN1:ΔG = -9.5KCalmol<sup>-1</sup>, STIM2 vs. MFN2:ΔG = -11.0KCalmol<sup>-1</sup>; STIM2 vs. OPA1:ΔG = -11.8KCalmol<sup>-1</sup>; ORAI1 vs. DNMI1L:ΔG = -20.0KCalmol<sup>-1</sup>, ORAI1 vs. FIS1:ΔG = -10.5KCalmol<sup>-1</sup>, ORAI1 vs. MFN1:ΔG = -11.7KCalmol<sup>-1</sup>, ORAI1 vs. MFN2:ΔG = -13.5KCalmol<sup>-1</sup>, ORAI1 vs. OPA1:ΔG = -11KCalmol<sup>-1</sup>; TRPC5 vs. DNMI1L:ΔG = -23.4KCalmol<sup>-1</sup>, TRPC5 vs. FIS1:ΔG = -22.7KCalmol<sup>-1</sup>, TRPC5 vs. MFN1:ΔG = -23.1KCalmol<sup>-1</sup>, TRPC5 vs. MFN2:ΔG = -22.8KCalmol<sup>-1</sup>, TRPC5 vs. OPA1:ΔG = -25.2KCalmol<sup>-1</sup> indicating higher chances of binding of SOC genes with proteins involved in mitochondrial dynamics (Figures 4Q–AJ). However, STRING analysis showed no known direct link between SOC genes and MDGs (Figures 5A–C).

### Survival Analysis

To understand the clinical relevance of these SOC genes, the correlation between gene expression versus overall survival and



**FIGURE 8 |** Survival analysis among Head neck cancer patients expressing altered levels of SOC in conjunction with MDGs. The survival data from TCGA was downloaded using TCGA biolinks package built for R statistical environment. The survival data for expression levels of each SOC in conjunction with MDGs is plotted.

relapse-free survival of HNSC patients were explored. Kaplan-Meier plotter was used to analyze overall survival analysis across TCGA-HNSC samples. The expression of STIM2, ORA11, TRPV1, TRPV2, TRPC1, TRPC3, TRPC5, TRPC6, TRPC7, and TRPM7 were found to be significantly ( $p < 0.05$ ) associated with HNSC patient survival (Figures 6A–O). The effect of expression of SOC along with MDGs on survival of

HNSC was visualized. Similar survival analysis was performed for relapse-free survival across TCGA data sets and are shown in Figures 7A–O. Next, the survival data were downloaded using TCGA biolinks via R programming. We analysed the survival probability for patients expressing SOC in conjunction with the MDGs and found that SOC along with MDGs are potential diagnostic and prognostic markers of HNSC (Figure 8).

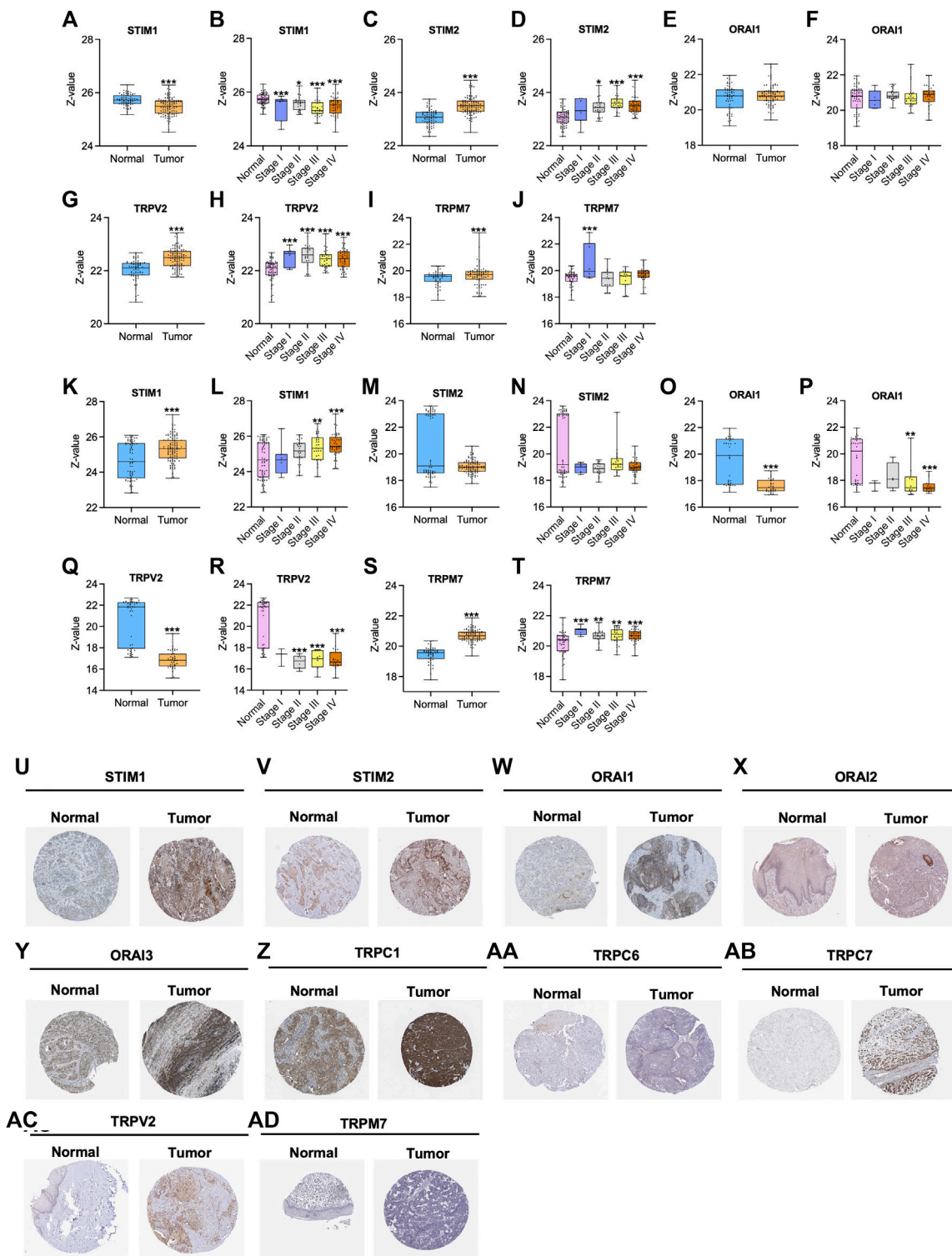


**FIGURE 9 |** Altered protein expression of SOC in HNSC. (A–J) The proteomics and (K–T) phosphoproteomics expression was downloaded from CPTAC-HNSC database using Python 3.0. The protein and phosphoprotein expression of SOC were plotted. The phosphoprotein sites which are considered to plot this graph include: S257 for STIM1; S261 for STIM2; T295 for ORAI1; S751 for TRPV2; S1477 for TRPM7. Asterisk represents  $p < 0.05$ ,  $** < 0.01$ ,  $*** < 0.001$  the statistical significance. (U–AD) Histopathology slides of tissue microarray were downloaded from Human Protein Atlas and the expression of the SOC are presented.

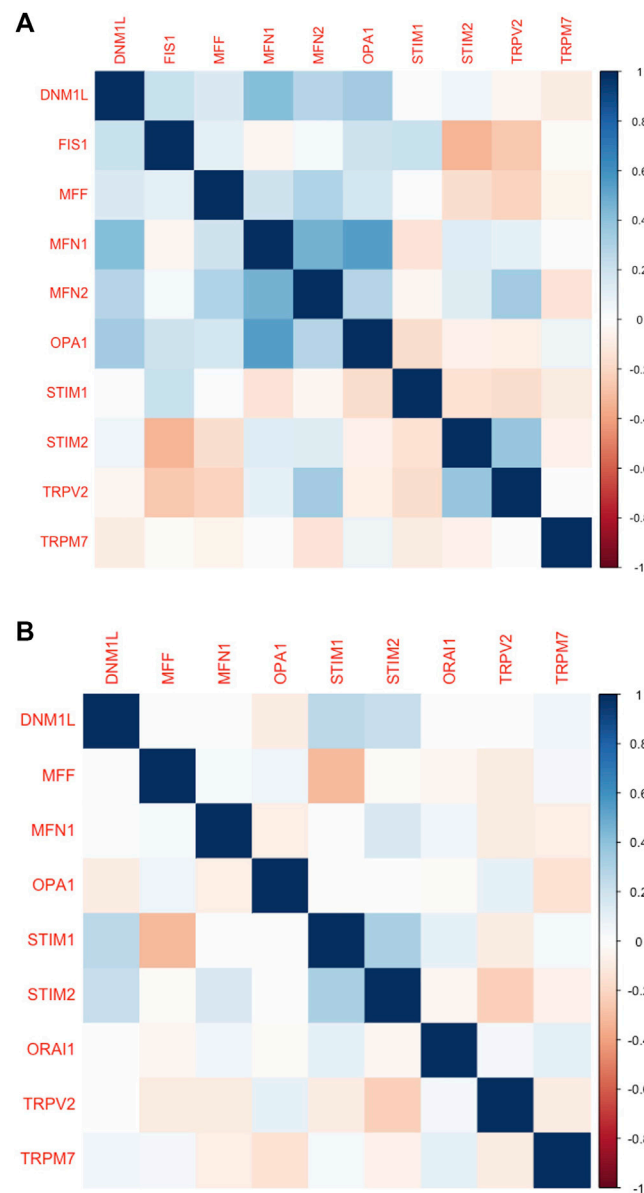


**FIGURE 10** | Protein levels of SOCs correlated with the MDGs in HNSC. **(A)** The proteomics and **(B)** phospho-proteomics expression CPTAC-HNSC data was downloaded using Python 3.0. The correlation was calculated and plotted using Corr plot package for R programming. The markings on right hand side indicates the color code for correlation coefficient.

## Expression of Store-Operated Calcium Channels and Their Correlation With Mitochondrial Dynamics Among Clinical Proteomic Tumor Analysis Consortium (CPTAC) and Gene Expression Omnibus (GEO) Datasets

Furthermore, we analysed the protein expression of SOCs and MDGs in HNSC. The proteomics, phosphoproteomics, and clinical data were obtained for CPTAC-HNSC using

Python version 3.0. The protein expression was available only for STIM1, STIM2, ORAI1, TRPV2, and TRPM7 in CPTAC dataset. This might be due to the spatio-temporal expression of proteins which is unrelated to the mRNA expression of genes. The available data were analyzed and visualized. The protein (**Figures 9A–J**) and phosphoprotein levels (**Figures 9K–T**) showed significant alteration of STIM1, STIM2, ORAI1, TRPV2, and TRPM7 in HNSC patients both overall and stage-wise compared to control samples. The histopathology slides downloaded from the

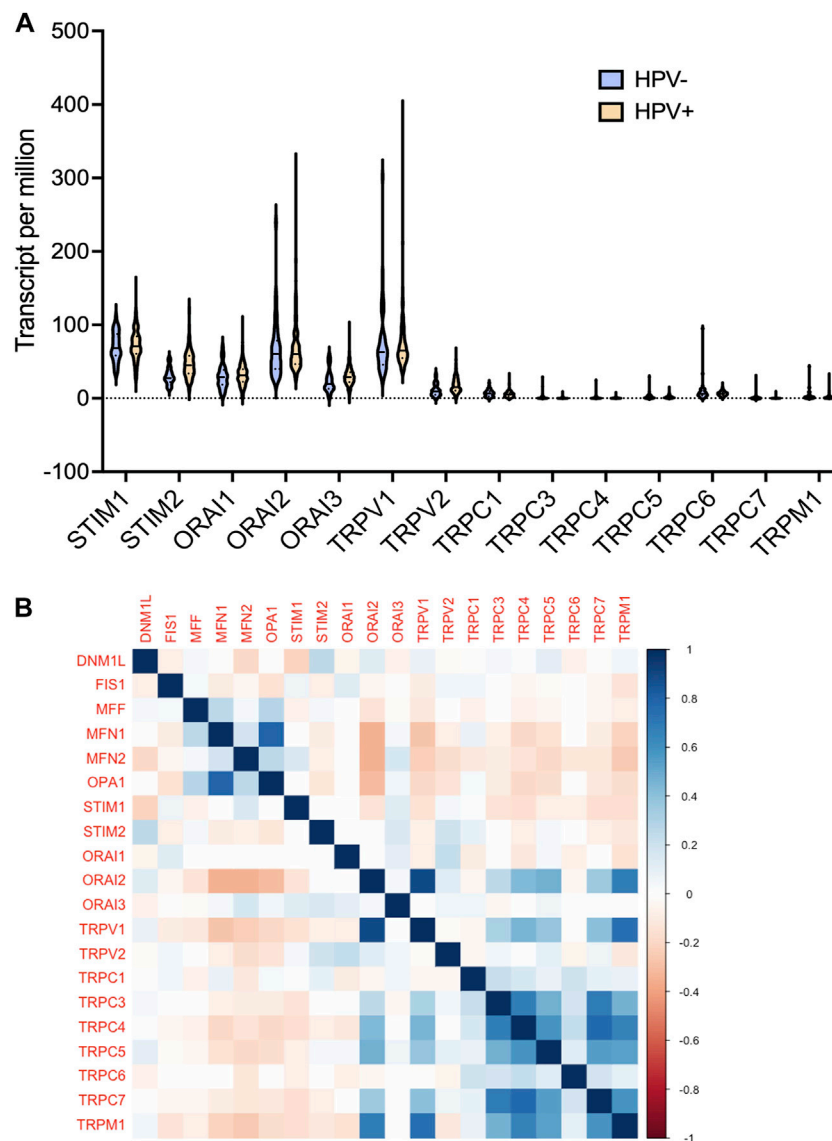
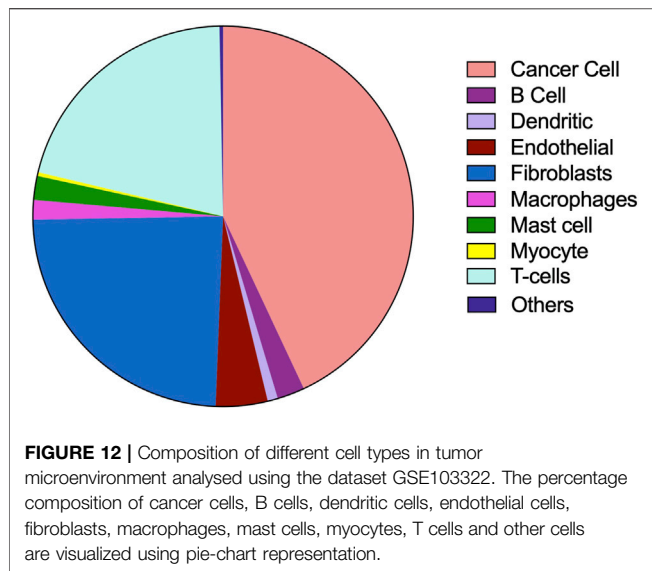


**FIGURE 11** | mRNA expression levels of SOC genes were correlated with the expression of MDGs in both HPV positive and negative HNSCs. The expression data from GSE17898 was downloaded from GEO datasets consisting total of 323 samples **(A)** The levels of SOC genes are plotted using Graphpad prism software and **(B)** correlation analysis was performed and plotted using Corr Plot package for R statistical environment. The gradation on the right side denote the correlation coefficient.

human protein atlas also showed similar results (Figures 9U–AD). Additionally, the correlation of SOC proteins and phosphoproteins with MD proteins were analyzed using Corr Plot package in R statistical environment (Figures 10A,B). In addition, the dataset GSE17898 consisting of normalized expression data from a total of 323 HNSC samples were downloaded and analyzed. The data showed remarkable alteration of SOC genes in both HPV positive and HPV negative samples (Figure 11A). The correlation analysis showed a significant association among SOC genes and MDGs expression which is in accordance with our TCGA and CPTAC analysis (Figure 11B).

## Single-Cell Gene Expression Analysis of Store-Operated Calcium Channels and Their Correlation With Mitochondrial Dynamics

The tumor microenvironment consists of heterogeneous population of cells contributing separately to the proliferation, development, metastasis, and therapeutic resistance (Da Silva-Diz et al., 2018; Stanta and Bonin, 2018; El-Sayes et al., 2021). Hence, we further analyzed single cell dataset for HNSC (GSE130922) downloaded from NCBI GEO datasets. Our analysis showed heterogeneous expression of SOC genes in different



cells of HNSC tumor tissues (Puram et al., 2017). The data was stratified across 10 different cell types- cancer cells and B cells, dendritic cells, endothelial cells, fibroblasts, macrophages, mast cells, monocytes, T-cells, and others among non-cancer stromal cells. The percentage population of these cells in the dataset are shown in **Figure 12**. STIM1, STIM2, ORAI1, ORAI2, ORAI3, TRPV1, TRPV2, and TRPM7 were found to be differentially expressed across all cell types in HNSC tumors (**Figures 13A-O**). Among the immune cells, STIM1 is expressed in all the immune cells with the highest expression in mast cells and lowest in dendritic and B cells. STIM2 and ORAI2 are expressed nearly equally in all the immune cells. ORAI1 levels were found to be nil in B cells. ORAI3 is found to be least expressed in dendritic and T cells. TRPC1, TRPC4, TRPC6, and TRPC7 are almost completely absent in all immune cells types whereas TRPC3 is expressed in T cells and dendritic cells, and TRPC5 is expressed only in T cells. TRPV1, TRPM1, and TRPM7 are almost equally expressed in all types of immune cells. TRPV2 is found to be expressed highly in macrophages. However, expression of ORAI2, TRPC5, and TRPV2 are high in B cells, T cells, and macrophages respectively compared to parenchymal cells. However, other SOCs are enriched in parenchymal cells including cancer cells compared to immune cells. In addition, SOCs were found to be highly expressed in cancer cells and fibroblasts among the parenchymal cells (**Figures 13A-O**). Further, a significant correlation of SOCs with MDGs were observed in cancer cells (**Figure 14**) and fibroblasts (**Figure 15**). The correlation coefficient and *p*-value are represented in the **Table 1**.

These single-cell analysis revealed the comprehensive role of SOCs together with MDGs in the tumor microenvironment.

Overall, our *in silico* approach depicted that SOCs might be involved in the regulation of mitochondrial function in HNSC and the expression of SOCs along with the MDGs can be a predictive marker of HNSC and might have prognostic value in these patients.

## DISCUSSION

Dysregulated intracellular  $Ca^{2+}$  signaling in cancer cells is shown to be remarkably associated with cancer cell growth, proliferation, angiogenesis, and metastasis (Barr et al., 2008; Chen et al., 2011; Wang et al., 2012; Bergmeier et al., 2013; Motiani et al., 2013; Wang et al., 2022). Dysregulation of SOCE and  $Ca^{2+}$  imbalance was reported in Sjögren's syndrome and in head and neck cancers treated with radiation (Cheng et al., 2012; Ambudkar, 2018). Elevated serum calcium levels is a proposed diagnostic marker for head and neck malignancy (Bradley and Hoskin, 2006). Recently, Newton et al. (2020) demonstrated that monoclonal antibody against PD-L1 enhances the functionality of T cells by modulating calcium release-activated calcium channels (Newton et al., 2020). siRNA-mediated knockdown of ORAI1 and STIM1 in Ca9-22 and OECM-1 oral cancer cell lines showed reduced proliferation, migration, and invasion of these cells (Wang et al., 2022). In the current study, we revealed that SOCs might be involved in regular mitochondrial function, and alteration in these might be a predictive and prognostic marker.

Substantial evidence has been provided in several different types of cells that SOCs are involved in cell interaction and secretory Ca-ATPase-2 pathway (Bergmeier et al., 2013). In addition, recent evidence suggests that the formation of a complex of these proteins with phosphatase calcineurin dephosphorylates cytoplasmic NFAT and induces nuclear translocation. Nuclear NFAT transcriptionally activates the expression of several genes including NANOG, OCT4, SOX2, and FGF19 which are involved in cancer cell stemness (Wang et al., 2021). In the current study, we conducted the gene ontology analysis, as a preliminary analysis to show the involvement of SOCs in the regulation of IP3 and ATPase pathways. Due to the involvement of SOCs in signaling pathways apart from their regular transport activities we hypothesized that SOCs might be involved even in the regulation of mitochondrial activities. Furthermore, disease ontology analysis was conducted to show the involvement of SOCs in several cancers.

Earlier studies have shown that the entry of  $Ca^{2+}$  ions through store-operated channels begins with the stimulation of plasma membrane receptors to phospholipase C and synthesis of inositol triphosphate. Activated SOCE aid in refilling  $Ca^{2+}$  stores for further stimulation (Putney, 1986; Parekh and Putney, 2005). In the current study, disease ontology analysis showed their involvement in inflammatory diseases, eye tumors, and medulloblastomas. This is in accordance with earlier *in vitro* studies (Wang et al., 2022). Subsequently, the TCGA-HNSC mRNA expression of SOCs showed that STIMs, ORAIs, TRPCs, TRPVs, and TRPMs are significantly altered in HNSC patients. The survival analysis clearly demonstrated that alteration in SOCs mRNA expression remarkably decreases the survival rate of these patients. Further, TCGA-HNSC based correlation analysis using Timer 2.0 tool showed a significant correlation in the expression of MDGs with SOCs. Mitochondrial regulation of SOCE is due to the

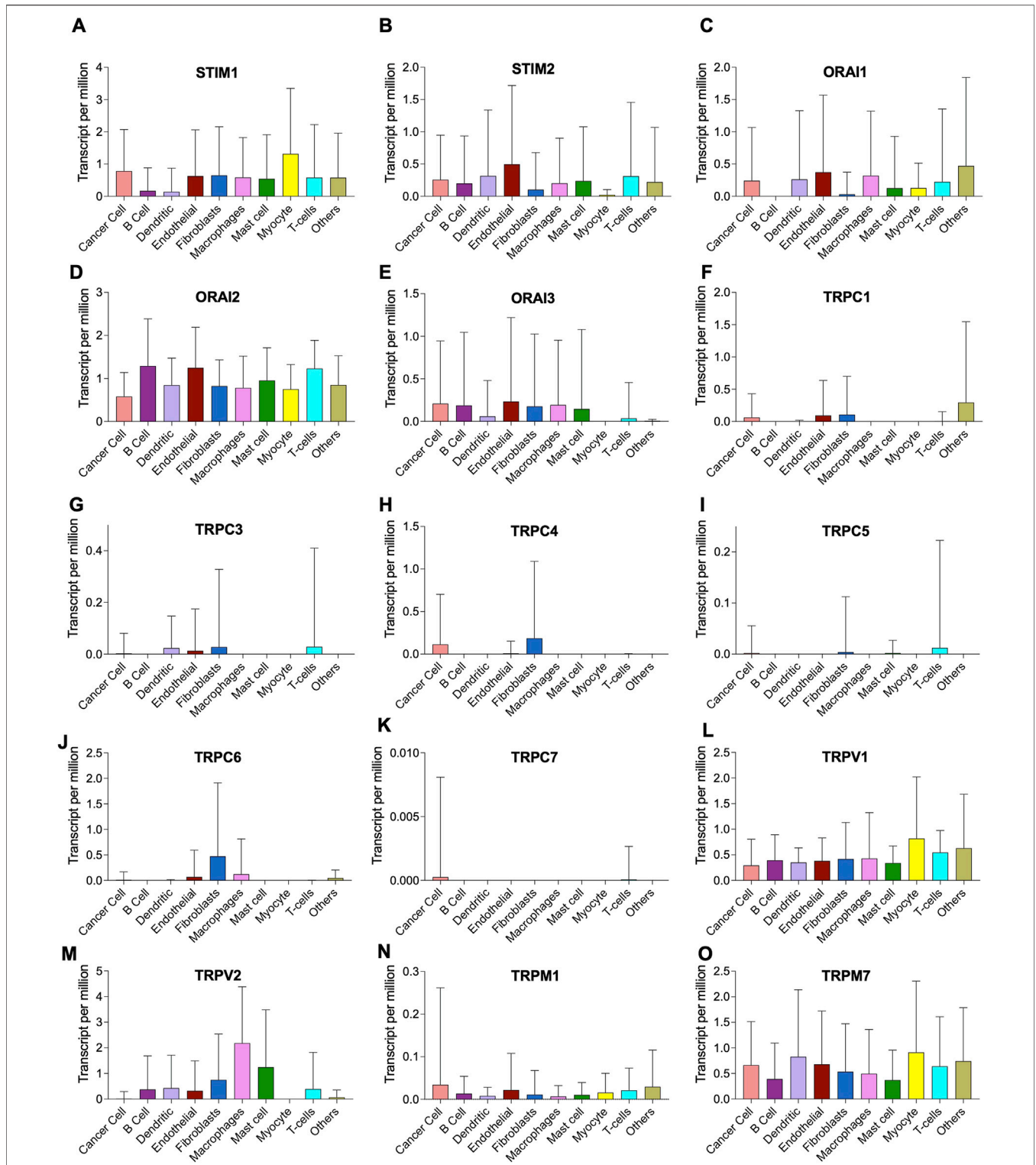
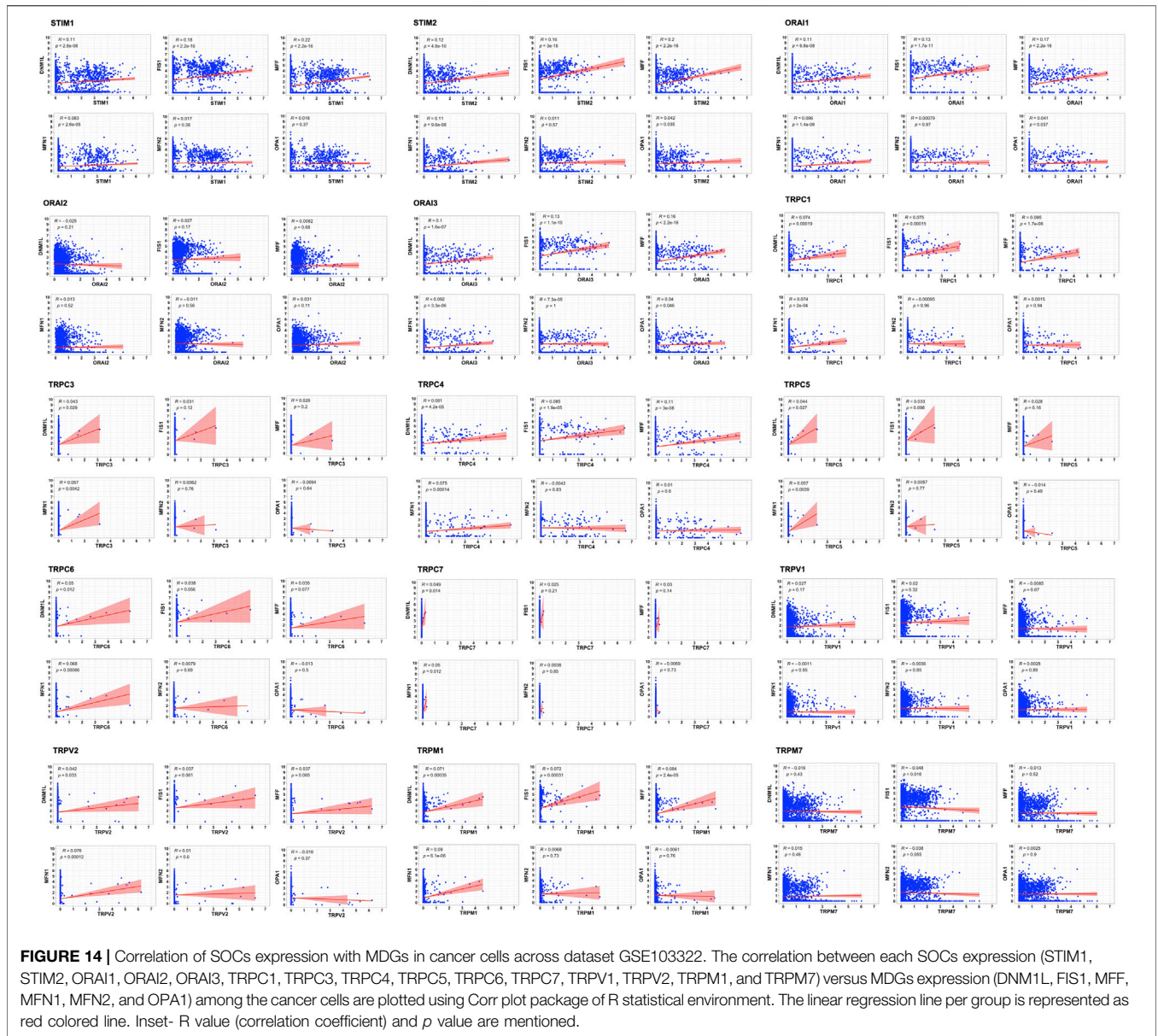
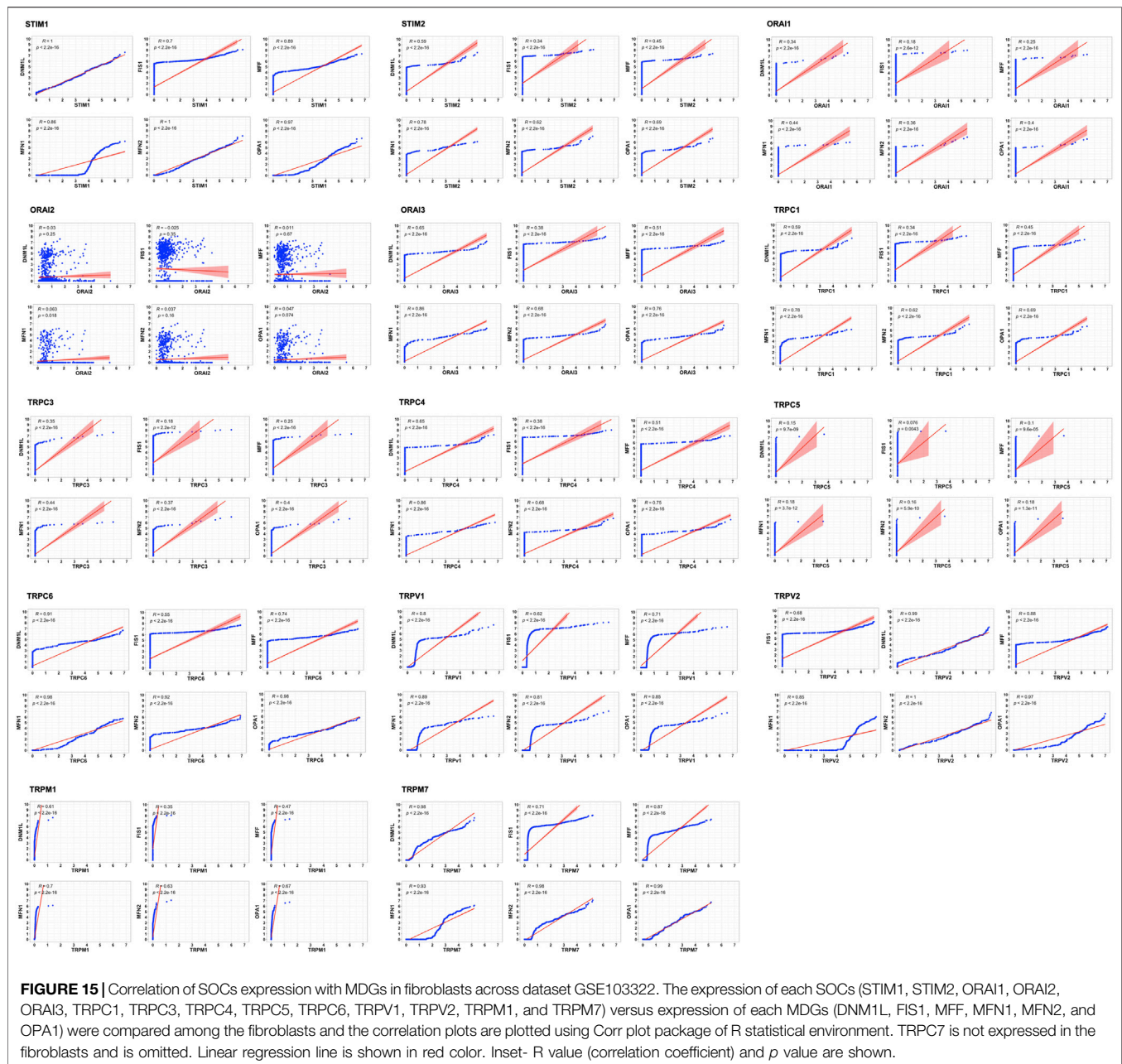


**FIGURE 13 |** Heterogenous expression of SOC in tumor microenvironment. **(A-O)** The expression data from GSE103322 comprising the data of 5,902 cells from 18 head and neck cancer tissues was downloaded from NCBI GEO website. The data comprised of different cell populations including cancer cells, B cells, dendritic cells, endothelial cells, fibroblasts, macrophages, mast cells, myocytes, T cells and other cells. The expression levels of each SOC in these different cell types are plotted using Graphpad prism software version 9.2.1.



ability to rapidly uptake the  $Ca^{2+}$  thus modulating the inositol phosphate mediated signaling. Hoth et al. (1997) showed that mitochondrial uncouplers inhibited  $Ca^{2+}$  exit from mitochondria leading to the prevention of sustained entry of  $Ca^{2+}$  into T-cells (Hoth et al., 1997). Further, Gilibert and Parekh revealed respiring mitochondria are required for  $Ca^{2+}$  homeostasis by CRAC channels (Gilibert and Parekh, 2000). In addition, FDA-approved drugs, leflunomide and teriflunomide were shown to be inhibitors of SOC in clinically-relevant doses in neuroblastoma cells (Rahman and Rahman, 2017). Miret-Casals et al. (2018) demonstrated that leflunomide and teriflunomide induces mitochondrial fusion through the activation of MFN2 in cervical cancer cell lines (Miret-Casals et al., 2018). Leflunomide has also been shown to promote

mitochondrial fusion via downregulating total and phospho DNM1L and inducing MFN2 leading to growth retardation in pancreatic adenocarcinoma cells (Yu et al., 2019). Recently, Yedida et al. (2019) demonstrated that apogossypol (a small molecule inhibitor of pan-Bcl2) mediated endoplasmic reticulum (ER) reorganization results in  $Ca^{2+}$  transfer between ER and mitochondria leading to inhibition of mitochondrial fission and apoptosis of HeLa cells (Yedida et al., 2019). This study also showed that leflunomide, a potent inhibitor of SOC, inhibits apogossypol-mediated ER reorganization and antagonizes its protective effect against apoptosis (Yedida et al., 2019). In accordance with these studies, our docking results showed higher negative binding energy for SOC with MDGs. To our knowledge, there are no *in vitro* or *in vivo*



studies showing the direct or indirect binding of SOC's with mitochondrial proteins. The STRING database also showed no known direct relation among these proteins. In the current study, we analyzed phosphoproteomic data for head and neck cancer from CPTAC. Mertins et al., 2016 integrated proteomics and phosphoproteomics data of CPTAC to identify distinct profiles in 77 genomically annotated breast tumors. In this study, the authors also revealed changes in phosphoproteomics of CDK12, PAK1, RIPK2, and TLK2. This study also proposed the phosphoproteomic changes in these proteins can be utilized as druggable kinases beyond HER2 (Mertins et al., 2016). Hence, we conducted the protein and phosphoprotein

analysis for clinical samples to show SOC proteins are also valuable biomarkers alongside the mRNA expression in head and neck cancers.

Among the post-translational modifications, phosphorylation of the protein is central to signaling mechanisms and is critical for various physiological responses. There are about 50,000 known phosphorylation sites that do not currently have any ascribed functions (Mayya and Han, 2009). However, quantitative phosphoproteomics has been an effective tool to identify functional phosphorylation sites and putative substrates of kinases. Immunoprecipitation followed by phosphoproteomics using mass spectrometry demonstrated

**TABLE 1 |** The correlation coefficient and *p*-value for SOC<sub>s</sub> and MDG<sub>s</sub> in cancer cells and fibroblasts.

Cell type	SOCs	MDGs	Correlation coefficient	<i>p</i> -Value	
Cancer cell	STIM1	DNM1L	0.11	$2.5 \times 10^{-8}$	
		FIS1	0.18	$<2.2 \times 10^{-16}$	
		MFF	0.22	$<2.2 \times 10^{-16}$	
	STIM2	MFN1	0.083	$2.6 \times 10^{-5}$	
		MFN2	0.017	0.38	
		OPA1	0.018	0.37	
		DNM1L	0.12	$4.8 \times 10^{-10}$	
		FIS1	0.16	$3 \times 10^{-15}$	
		MFF	0.2	$<2.2 \times 10^{-16}$	
	ORAI1	MFN1	0.11	$9.6 \times 10^{-8}$	
		MFN2	0.011	0.57	
		OPA1	0.042	0.035	
		DNM1L	0.11	$6.8 \times 10^{-8}$	
		FIS1	0.13	$1.7 \times 10^{-11}$	
		MFF	0.17	$<2.2 \times 10^{-16}$	
		MFN1	0.096	$1.4 \times 10^{-6}$	
		MFN2	0.00079	0.97	
		OPA1	0.041	0.037	
		ORAI2	DNM1L	-0.025	0.21
	FIS1		0.027	0.17	
	MFF		0.0082	0.68	
	MFN1		0.013	0.52	
	MFN2		-0.011	0.56	
	OPA1		0.031	0.11	
	DNM1L		0.1	$1.6 \times 10^{-7}$	
	ORAI3	FIS1	0.13	$1.1 \times 10^{-10}$	
		MFF	0.16	$2.2 \times 10^{-16}$	
		MFN1	0.092	$3.3 \times 10^{-6}$	
		MFN2	$7.3 \times 10^{-5}$	1	
		OPA1	0.04	0.046	
		TRPC1	DNM1L	0.074	0.00019
			FIS1	0.075	0.00015
			MFF	0.095	$1.7 \times 10^{-6}$
			MFN1	0.074	$2 \times 10^{-4}$
			MFN2	-0.00095	0.96
	OPA1		0.0015	0.94	
	DNM1L		0.043	0.029	
	TRPC3	FIS1	0.031	0.12	
		MFF	0.026	0.2	
		MFN1	0.057	0.0042	
		MFN2	0.0062	0.76	
		OPA1	-0.0094	0.64	
		TRPC4	DNM1L	0.081	$4.2 \times 10^{-5}$
			FIS1	0.085	$1.9 \times 10^{-5}$
	MFF		0.11	$3 \times 10^{-8}$	
	MFN1		0.075	0.00014	
	MFN2		-0.0043	0.83	
	TRPC5	OPA1	0.01	0.6	
		DNM1L	0.044	0.027	
		FIS1	0.033	0.098	
		MFF	0.028	1.6	
		MFN1	0.057	0.0039	
	TRPC6	MFN2	0.0057	0.77	
		OPA1	-0.014	0.49	
		DNM1L	0.05	0.012	
		FIS1	0.038	0.056	
		MFF	0.035	0.077	
		MFN1	0.068	0.00066	
		MFN2	0.0079	0.69	
	TRPC7	OPA1	-0.013	0.5	
		DNM1L	0.049	0.14	
		FIS1	0.025	0.21	
			MFF	0.03	0.14

(Continued in next column)

**TABLE 1 |** (Continued) The correlation coefficient and *p*-value for SOC<sub>s</sub> and MDG<sub>s</sub> in cancer cells and fibroblasts.

Cell type	SOCs	MDGs	Correlation coefficient	<i>p</i> -Value		
Cancer cell	TRPV1	MFN1	0.05	0.012		
		MFN2	0.0038	0.85		
		OPA1	-0.0069	0.73		
		DNM1L	0.027	0.17		
		FIS1	0.02	0.32		
		MFF	-0.0085	0.67		
		MFN1	-0.0011	0.95		
		MFN2	-0.0036	0.85		
		OPA1	0.0028	0.89		
		TRPV2	DNM1L	0.042	0.033	
			FIS1	0.031	0.06	
			MFF	0.037	0.065	
			MFN1	0.076	0.00012	
			MFN2	0.01	0.6	
			OPA1	-0.018	0.37	
	DNM1L		0.071	0.00035		
	TRPM1	FIS1	0.072	0.00031		
		MFF	0.084	$2.4 \times 10^{-5}$		
		MFN1	0.09	$6.1 \times 10^{-6}$		
		MFN2	-0.0068	0.73		
		OPA1	-0.0061	0.76		
		TRPM7	DNM1L	-0.016	0.43	
			FIS1	-0.048	0.016	
			MFF	-0.013	0.52	
			MFN1	0.015	0.46	
			MFN2	-0.038	0.055	
	OPA1		0.0025	0.9		
	Fibroblasts	STIM1	DNM1L	1	$<2.2 \times 10^{-16}$	
			FIS1	0.7	$<2.2 \times 10^{-16}$	
			MFF	0.89	$<2.2 \times 10^{-16}$	
		STIM2	MFN1	0.86	$<2.2 \times 10^{-16}$	
			MFN2	1	$<2.2 \times 10^{-16}$	
			OPA1	0.97	$<2.2 \times 10^{-16}$	
			DNM1L	0.59	$<2.2 \times 10^{-16}$	
			FIS1	0.34	$<2.2 \times 10^{-16}$	
			MFF	0.45	$<2.2 \times 10^{-16}$	
			MFN1	0.78	$<2.2 \times 10^{-16}$	
			MFN2	0.62	$<2.2 \times 10^{-16}$	
			OPA1	0.69	$<2.2 \times 10^{-16}$	
			ORAI1	DNM1L	0.34	$<2.2 \times 10^{-16}$
				FIS1	0.18	$=2.2 \times 10^{-16}$
				MFF	0.25	$<2.2 \times 10^{-16}$
				MFN1	0.44	$<2.2 \times 10^{-16}$
				MFN2	0.36	$<2.2 \times 10^{-16}$
OPA1				0.4	$<2.2 \times 10^{-16}$	
DNM1L		0.03		0.25		
ORAI2		FIS1	-0.025	0.35		
		MFF	0.011	0.67		
		MFN1	0.063	0.018		
		MFN2	0.037	0.16		
		OPA1	0.047	0.074		
		ORAI3	DNM1L	0.65	$<2.2 \times 10^{-16}$	
			FIS1	0.38	$<2.2 \times 10^{-16}$	
			MFF	0.51	$<2.2 \times 10^{-16}$	
		TRPC1	MFN1	0.86	$<2.2 \times 10^{-16}$	
			MFN2	0.68	$<2.2 \times 10^{-16}$	
OPA1			0.76	$<2.2 \times 10^{-16}$		
DNM1L			0.59	$<2.2 \times 10^{-16}$		
FIS1			0.34	$<2.2 \times 10^{-16}$		
MFF			0.45	$<2.2 \times 10^{-16}$		
MFN1			0.78	$<2.2 \times 10^{-16}$		
MFN2			0.62	$<2.2 \times 10^{-16}$		

(Continued on following page)

**TABLE 1 |** (Continued) The correlation coefficient and *p*-value for SOCs and MDGs in cancer cells and fibroblasts.

Cell type	SOCs	MDGs	Correlation coefficient	<i>p</i> -Value
TRPC3		OPA1	0.69	$<2.2 \times 10^{-16}$
		DNM1L	0.35	$<2.2 \times 10^{-16}$
		FIS1	0.18	$<2.2 \times 10^{-16}$
		MFF	0.25	$<2.2 \times 10^{-16}$
		MFN1	0.44	$<2.2 \times 10^{-16}$
TRPC4		MFN2	0.37	$<2.2 \times 10^{-16}$
		OPA1	0.4	$<2.2 \times 10^{-16}$
		DNM1L	0.65	$<2.2 \times 10^{-16}$
		FIS1	0.38	$<2.2 \times 10^{-16}$
		MFF	0.51	$<2.2 \times 10^{-16}$
TRPC5		MFN1	0.86	$<2.2 \times 10^{-16}$
		MFN2	0.68	$<2.2 \times 10^{-16}$
		OPA1	0.75	$<2.2 \times 10^{-16}$
		DNM1L	0.15	$9.7 \times 10^{-9}$
		FIS1	0.076	0.0043
TRPC6		MFF	0.1	$<2.2 \times 10^{-16}$
		MFN1	0.18	$3.7 \times 10^{-12}$
		MFN2	0.16	$5.9 \times 10^{-10}$
		OPA1	0.18	$1.3 \times 10^{-11}$
		DNM1L	0.91	$<2.2 \times 10^{-16}$
TRPV1		FIS1	0.55	$<2.2 \times 10^{-16}$
		MFF	0.74	$<2.2 \times 10^{-16}$
		MFN1	0.98	$<2.2 \times 10^{-16}$
		MFN2	0.92	$<2.2 \times 10^{-16}$
		OPA1	0.98	$<2.2 \times 10^{-16}$
TRPV2		DNM1L	0.8	$<2.2 \times 10^{-16}$
		FIS1	0.62	$<2.2 \times 10^{-16}$
		MFF	0.71	$<2.2 \times 10^{-16}$
		MFN1	0.89	$<2.2 \times 10^{-16}$
		MFN2	0.81	$<2.2 \times 10^{-16}$
TRPM1		OPA1	0.85	$<2.2 \times 10^{-16}$
		DNM1L	0.68	$<2.2 \times 10^{-16}$
		FIS1	0.99	$<2.2 \times 10^{-16}$
		MFF	0.88	$<2.2 \times 10^{-16}$
		MFN1	0.85	$<2.2 \times 10^{-16}$
TRPM7		MFN2	1	$<2.2 \times 10^{-16}$
		OPA1	0.97	$<2.2 \times 10^{-16}$
		DNM1L	0.61	$<2.2 \times 10^{-16}$
		FIS1	0.35	$<2.2 \times 10^{-16}$
		MFF	0.47	$<2.2 \times 10^{-16}$
		MFN1	0.7	$<2.2 \times 10^{-16}$
		MFN2	0.63	$<2.2 \times 10^{-16}$
		OPA1	0.67	$<2.2 \times 10^{-16}$
		DNM1L	0.98	$<2.2 \times 10^{-16}$
		FIS1	0.71	$<2.2 \times 10^{-16}$
		MFF	0.87	$<2.2 \times 10^{-16}$
		MFN1	0.93	$<2.2 \times 10^{-16}$
		MFN2	0.98	$<2.2 \times 10^{-16}$
		OPA1	0.99	$<2.2 \times 10^{-16}$

that RTKs including ALK, ROS fusion proteins, PDGFR $\alpha$ , and DDR were found to be highly phosphorylated in non-small cell lung carcinoma cell lines and tumor samples (Rikova et al., 2007). Recently, phosphotyrosine directed mass spectrometry analysis conducted by Van Linde et al. (2022) showed the complex kinase activities in glioblastoma. The study suggested the potential of phosphoproteomic analysis for the identification of targets for the treatment modalities (Van Linde et al., 2022). In the current study, analysis of the protein and phosphoprotein expression of SOCs were

crucial to show that they might be involved in the regulation of mitochondrial dynamic changes. Also, high levels of phosphoprotein expression of SOCs indicate their activity in head and neck cancers. Further, the CPTAC-HNSC dataset revealed a significant correlation in the expression of SOCs with MDGs. The survival correlation analysis indicated that the patients expressing altered levels of SOCs along with MDGs possess less survival probability compared with those who are expressing normal levels of either SOCs or MDGs. This indicated that the evaluation of SOCs combined with MDGs might be a potential biomarker in HNSCs.

Furthermore, single-cell analysis showed heterogeneity in the expression of SOCs across the ten different cell types. The co-culture of mouse embryonic fibroblasts with MDA-MB-231 by Yang and Huang (2005) showed the critical role of Ca<sup>2+</sup> ions influx in fibroblast cells migration (Yang and Huang, 2005). In addition, Davis et al. (2012) demonstrated that altered function of ORAI1 and TRPC1 led to EGF-induced EMT changes in triple-negative breast cancer cell lines (Davis et al., 2012). More recently, Zhang et al. (2020) revealed serum- and glucocorticoid-inducible kinase 1 (SGK1) regulates osteoclastogenesis via controlling ORAI1 leading to bone metastasis of breast cancer both in *in vitro* and *in vivo* models (Zhang et al., 2020). In accordance with these results, single-cell analysis described that the expression of SOCs were found to be strongly correlated with the expression of MDGs in cancer cells and fibroblasts indicating the role of SOCs in conjunction with mitochondrial dysfunction in driving the cancer cell hallmarks. Additionally, our analysis showed the critical role of tumor heterogeneity in the progression of cancer and highlights the importance of developing targeted therapy for the microenvironment niche. However, further studies need to be conducted to validate the role of differential expression of SOC in the different cell populations of the tumor tissue.

Taken together, these results indicated that SOCs and MDGs combined alteration might be a potential diagnostic and prognostic marker in HNSC.

## CONCLUSION

Our *in silico* analysis shows the altered mRNA and protein expression of SOCs in head and neck cancer and suggests their role as possible biomarkers. We also showed a strong correlation in the expression of MDGs with SOCs in TCGA-HNSC, CPTAC-HNSC, GSE171898, and GSE103322 datasets. We showed for the first time that the SOCs binds to MDGs with very high efficiency. Mechanistic studies need to be conducted further to validate their role in mitochondrial dysfunction and in HNSC development. Based on our *in silico* studies we propose that the expression of SOCs along with MDGs might serve as a better early diagnostic and prognostic marker in HNSC patients. However, further studies need to be conducted to evaluate their potential use in clinical diagnosis and management.

## DATA AVAILABILITY STATEMENT

Publicly available datasets were analyzed in this study. This data can be found here: NCBI Gene Expression Omnibus.

## AUTHOR CONTRIBUTIONS

MH: Conceptualization, Methodology, Data Curation, Formal analysis, Investigation, Manuscript preparation, Visualization, UD: Confirmation of data, Editing, Visualization, SJ: Overall review and editing, AS: Overall review and editing AC: Methodology, Software, Resources, SA: Methodology, Resources, Revision, MS: Methodology, Resources, Revision, AK: Conceptualization, Supervision, Proof reading, Project administration, Funding acquisition.

## FUNDING

This project was supported by BT/556/NE/U-Excel/2016 grant awarded to AK by Department of Biotechnology (DBT), Government of India. This work was also supported by the

## REFERENCE

- Alptekin, M., Eroglu, S., Tutar, E., Sencan, S., Geyik, M. A., Ulasli, M., et al. (2015). Gene Expressions of TRP Channels in Glioblastoma Multiforme and Relation with Survival. *Tumor Biol.* 36, 9209–9213. doi:10.1007/s13277-015-3577-x
- Ambudkar, I. (2018). Calcium Signaling Defects Underlying Salivary Gland Dysfunction. *Biochimica Biophysica Acta (BBA) - Mol. Cell. Res.* 1865, 1771–1777. doi:10.1016/j.bbamcr.2018.07.002
- Authi, K. S. (2007). TRP Channels in Platelet Function. *Handb. Exp. Pharmacol.* 179, 425–443. doi:10.1007/978-3-540-34891-7\_25
- Barr, V. A., Bernot, K. M., Srikanth, S., Gwack, Y., Balagopalan, L., Regan, C. K., et al. (2008). Dynamic Movement of the Calcium Sensor STIM1 and the Calcium Channel Orai1 in Activated T-Cells: Puncta and Distal Caps. *MBoC* 19, 2802–2817. doi:10.1091/mbc.e08-02-0146
- Bastián-Eugenio, C. E., Bohórquez-Hernández, A., Pacheco, J., Sampieri, A., Asanov, A., Ocelotl-Oviedo, J. P., et al. (2019). Heterologous Calcium-dependent Inactivation of Orail by Neighboring TRPV1 Channels Modulates Cell Migration and Wound Healing. *Commun. Biol.* 2, 88. doi:10.1038/s42003-019-0338-1
- Bergmeier, W., Weidinger, C., Zee, I., and Feske, S. (2013). Emerging Roles of Store-Operated Ca<sup>2+</sup>-entry through STIM and ORAI Proteins in Immunity, Hemostasis and Cancer. *Channels* 7, 379–391. doi:10.4161/chan.24302
- Berman, H. M., Westbrook, J., Feng, Z., Gilliland, G., Bhat, T. N., Weissig, H., et al. (2000). The Protein Data Bank. *Nucleic Acids Res.* 28, 235–242. doi:10.1093/nar/28.1.235
- Berridge, M. J., Bootman, M. D., and Roderick, H. L. (2003). Calcium Signalling: Dynamics, Homeostasis and Remodelling. *Nat. Rev. Mol. Cell. Biol.* 4, 517–529. doi:10.1038/nrm1155
- Bradley, P. J., and Hoskin, D. (2006). Hyercalcaemia in Head and Neck Squamous Cell Carcinoma. *Curr. Opin. Otolaryngol. Head. Neck Surg.* 14, 51–54. doi:10.1097/01.moo.0000193176.54450.c4
- Cao, Y.-L., Meng, S., Chen, Y., Feng, J.-X., Gu, D.-D., Yu, B., et al. (2017). MFN1 Structures Reveal Nucleotide-Triggered Dimerization Critical for Mitochondrial Fusion. *Nature* 542, 372–376. doi:10.1038/nature21077
- Cerami, E., Gao, J., Dogrusoz, U., Gross, B. E., Sumer, S. O., Aksoy, B. A., et al. (2012). The cBio Cancer Genomics Portal: An Open Platform for Exploring Multidimensional Cancer Genomics Data: Figure 1. *Cancer Discov.* 2, 401–404. doi:10.1158/2159-8290.cd-12-0095
- Chang, Y., Roy, S., and Pan, Z. (2021). Store-Operated Calcium Channels as Drug Target in Gastroesophageal Cancers. *Front. Pharmacol.* 12, 668730. doi:10.3389/fphar.2021.668730

Researchers Supporting Project number (RSP-2022/5) King Saud University, Riyadh, Saudi Arabia.

## ACKNOWLEDGMENTS

MH acknowledges Science and Engineering Board (SERB)-National Post-Doctoral Fellowship (N-PDF) (PDF/2021/004053) for the financial support. UD acknowledges Prime Minister's Research Fellowship (PMRF) program, Ministry of Education (MoE), Govt. of India for providing her the prestigious fellowship.

## SUPPLEMENTARY MATERIAL

The Supplementary Material for this article can be found online at: <https://www.frontiersin.org/articles/10.3389/fgene.2022.866473/full#supplementary-material>

**Supplementary Figure 1** | Graphical Abstract.

- Chen, Y.-F., Chiu, W.-T., Chen, Y.-T., Lin, P.-Y., Huang, H.-J., Chou, C.-Y., et al. (2011). Calcium Store Sensor Stromal-Interaction Molecule 1-dependent Signaling Plays an Important Role in Cervical Cancer Growth, Migration, and Angiogenesis. *Proc. Natl. Acad. Sci. U.S.A.* 108, 15225–15230. doi:10.1073/pnas.1103315108
- Cheng, K. T., Alevizos, I., Liu, X., Swaim, W. D., Yin, H., Feske, S., et al. (2012). STIM1 and STIM2 Protein Deficiency in T Lymphocytes Underlies Development of the Exocrine Gland Autoimmune Disease, Sjögren's Syndrome. *Proc. Natl. Acad. Sci. U.S.A.* 109, 14544–14549. doi:10.1073/pnas.1207354109
- Da Silva-Diz, V., Lorenzo-Sanz, L., Bernat-Peguera, A., Lopez-Cerda, M., and Muñoz, P. (2018). Cancer Cell Plasticity: Impact on Tumor Progression and Therapy Response. *Seminars Cancer Biol.* 53, 48–58. doi:10.1016/j.semcancer.2018.08.009
- Davis, F. M., Peters, A. A., Grice, D. M., Cabot, P. J., Parat, M.-O., Roberts-Thomson, S. J., et al. (2012). Non-stimulated, Agonist-Stimulated and Store-Operated Ca<sup>2+</sup> Influx in MDA-MB-468 Breast Cancer Cells and the Effect of EGF-Induced EMT on Calcium Entry. *PLoS One* 7, e36923. doi:10.1371/journal.pone.0036923
- Desta, I. T., Porter, K. A., Xia, B., Kozakov, D., and Vajda, S. (2020). Performance and its Limits in Rigid Body Protein-Protein Docking. *Structure* 28, 1071–1081. doi:10.1016/j.str.2020.06.006
- El-Sayes, N., Vito, A., and Mossman, K. (2021). Tumor Heterogeneity: A Great Barrier in the Age of Cancer Immunotherapy. *Cancers (Basel)* 13, 806. doi:10.3390/cancers13040806
- Feske, S. (2019). CRAC Channels and Disease - from Human CRAC Channelopathies and Animal Models to Novel Drugs. *Cell. Calcium* 80, 112–116. doi:10.1016/j.ceca.2019.03.004
- Gilbert, J. A., and Parekh, A. B. (2000). Respiring Mitochondria Determine the Pattern of Activation and Inactivation of the Store-Operated Ca(2+) Current I(CRAC). *Embo J.* 19, 6401–6407. doi:10.1093/emboj/19.23.6401
- Guldani, R., De Clippele, M., Ratbi, I., Gailly, P., and Tadjeddine, N. (2019). Store-Operated Calcium Entry Contributes to Cisplatin-Induced Cell Death in Non-small Cell Lung Carcinoma. *Cancers (Basel)* 11, 430. doi:10.3390/cancers11030430
- Hernández-Morales, M., Sobradillo, D., Valero, R. A., Muñoz, E., Ubierna, D., Moyer, M. P., et al. (2017). Mitochondria Sustain Store-Operated Currents in Colon Cancer Cells but Not in Normal Colonic Cells: Reversal by Non-steroidal Anti-inflammatory Drugs. *Oncotarget* 8, 55332–55352. doi:10.18632/oncotarget.19430
- Hoth, M., Fanger, C. M., and Lewis, R. S. (1997). Mitochondrial Regulation of Store-Operated Calcium Signaling in T Lymphocytes. *J. Cell. Biol.* 137, 633–648. doi:10.1083/jcb.137.3.633

- Huang, C., Chen, L., Savage, S. R., Eiguez, R. V., Dou, Y., Li, Y., et al. (2021). Proteogenomic Insights into the Biology and Treatment of HPV-Negative Head and Neck Squamous Cell Carcinoma. *Cancer Cell* 39, 361–379. doi:10.1016/j.ccell.2020.12.007
- Jiang, J., Li, M.-H., Inoue, K., Chu, X.-P., Seeds, J., and Xiong, Z.-G. (2007). Transient Receptor Potential Melastatin 7-like Current in Human Head and Neck Carcinoma Cells: Role in Cell Proliferation. *Cancer Res* 67, 10929–10938. doi:10.1158/0008-5472.can-07-1121
- Kanehisa, M., and Goto, S. (2000). KEGG: Kyoto Encyclopedia of Genes and Genomes. *Nucleic Acids Res* 28, 27–30. doi:10.1093/nar/28.1.27
- Khan, H. Y., Mpilla, G. B., Sexton, R., Viswanadha, S., Penmetsa, K. V., Aboukameel, A., et al. (2020). Calcium Release-Activated Calcium (CRAC) Channel Inhibition Suppresses Pancreatic Ductal Adenocarcinoma Cell Proliferation and Patient-Derived Tumor Growth. *Cancers (Basel)* 12, 750. doi:10.3390/cancers12030750
- Kishida, H., and Sugio, S. (2013). Crystal Structure of GTPase Domain Fused with Minimal Stalks from Human Dynamin-1-like Protein (Dlp1) in Complex with Several Nucleotide Analogues. *Curr. Top. Pept. Protein Res* 14, 67–77.
- Kozakov, D., Beglov, D., Bohnuud, T., Mottarella, S. E., Xia, B., Hall, D. R., et al. (2013). How Good Is Automated Protein Docking? *Proteins* 81, 2159–2166. doi:10.1002/prot.24403
- Kozakov, D., Hall, D. R., Xia, B., Porter, K. A., Padhorney, D., Yueh, C., et al. (2017). The ClusPro Web Server for Protein-Protein Docking. *Nat. Protoc.* 12, 255–278. doi:10.1038/nprot.2016.169
- Lánczky, A., and Györfi, B. (2021). Web-Based Survival Analysis Tool Tailored for Medical Research (KMplot): Development and Implementation. *J. Med. Internet Res* 23, e27633. doi:10.2196/27633
- Lewis, R. S. (2007). The Molecular Choreography of a Store-Operated Calcium Channel. *Nature* 446, 284–287. doi:10.1038/nature05637
- Li, T., Fu, J., Zeng, Z., Cohen, D., Li, J., Chen, Q., et al. (2020). TIMER2.0 for Analysis of Tumor-Infiltrating Immune Cells. *Nucleic Acids Res* 48, W509–w514. doi:10.1093/nar/gkaa407
- Li, Y.-J., Cao, Y.-L., Feng, J.-X., Qi, Y., Meng, S., Yang, J.-F., et al. (2019). Structural Insights of Human Mitofusin-2 into Mitochondrial Fusion and CMT2A Onset. *Nat. Commun.* 10, 4914. doi:10.1038/s41467-019-12912-0
- Liu, X., Liu, P., Chernock, R. D., Kuhs, K. A. L., Lewis, J. S., Jr., Luo, J., et al. (2020). A Prognostic Gene Expression Signature for Oropharyngeal Squamous Cell Carcinoma. *EBioMedicine* 61, 102805. doi:10.1016/j.ebiom.2020.102805
- Liu, Y., Zheng, X., Mueller, G. A., Sobhany, M., Derose, E. F., Zhang, Y., et al. (2012). Crystal Structure of Calmodulin Binding Domain of Orai1 in Complex with Ca<sup>2+</sup>/Calmodulin Displays a Unique Binding Mode. *J. Biol. Chem.* 287, 43030–43041. doi:10.1074/jbc.m112.380964
- Ma, X., Cheng, K.-T., Wong, C.-O., O'Neil, R. G., Birnbaumer, L., Ambudkar, I. S., et al. (2011). Heteromeric TRPV4-C1 Channels Contribute to Store-Operated Ca<sup>2+</sup> Entry in Vascular Endothelial Cells. *Cell. Calcium* 50, 502–509. doi:10.1016/j.ceca.2011.08.006
- Mayya, V., and Han, D. K. (2009). Phosphoproteomics by Mass Spectrometry: Insights, Implications, Applications and Limitations. *Expert Rev. Proteomics* 6, 605–618. doi:10.1586/epr.09.84
- Mertins, P., Mani, D. R., Ruggles, K. V., Gillette, M. A., Clauser, K. R., Wang, P., et al. (2016). Proteogenomics Connects Somatic Mutations To Signalling In Breast Cancer. *Nature* 534, 55–62. doi:10.1038/nature18003
- Míret-Casals, L., Sebastián, D., Brea, J., Rico-Leo, E. M., Palacín, M., Fernández-Salguero, P. M., et al. (2018). Identification of New Activators of Mitochondrial Fusion Reveals a Link between Mitochondrial Morphology and Pyrimidine Metabolism. *Cell. Chem. Biol.* 25, 268–278. doi:10.1016/j.chembiol.2017.12.001
- Motiani, R. K., Hyzinski-García, M. C., Zhang, X., Henkel, M. M., Abdullaev, I. F., Kuo, Y.-H., et al. (2013). STIM1 and Orai1 Mediate CRAC Channel Activity and Are Essential for Human Glioblastoma Invasion. *Pflugers Arch. - Eur. J. Physiol.* 465, 1249–1260. doi:10.1007/s00424-013-1254-8
- Nagy, Á., Munkácsy, G., and Györfi, B. (2021). Pancancer Survival Analysis Of Cancer Hallmark Genes. *Sci. Rep.* 11, 6047. doi:10.1038/s41598-021-84787-5
- Newton, H. S., Gawali, V. S., Chimote, A. A., Lehn, M. A., Palackdharry, S. M., Hinrichs, B. H., et al. (2020). PD1 Blockade Enhances K<sup>+</sup> Channel Activity, Ca<sup>2+</sup> Signaling, and Migratory Ability in Cytotoxic T Lymphocytes of Patients with Head and Neck Cancer. *J. Immunother. Cancer* 8, e000844. doi:10.1136/jitc-2020-000844
- Oell-Kotikangas, H., Schwab, U., Österlund, P., Saarihahti, K., Mäkitie, O., and Mäkitie, A. A. (2012). High Prevalence of Vitamin D Insufficiency in Patients with Head And Neck Cancer at Diagnosis. *Head Neck* 34, 1450–1455. doi:10.1002/hed.21954
- Mounir, M., Lucchetta, M., Silva, T. C., Olsen, C., Bontempi, G., Chen, X., et al. (2019). New Functionalities in the TCGAAbiolinks Package for the Study and Integration of Cancer Data from GDC and GTEx. *PLoS Comput. Biol.* 15, e1006701. doi:10.1371/journal.pcbi.1006701
- Parekh, A. B., and Putney, J. W., Jr. (2005). Store-operated Calcium Channels. *Physiol. Rev.* 85, 757–810. doi:10.1152/physrev.00057.2003
- Puram, S. V., Tirosh, I., Parkh, A. S., Patel, A. P., Yizhak, K., Gillespie, S., et al. (2017). Single-Cell Transcriptomic Analysis of Primary and Metastatic Tumor Ecosystems in Head and Neck Cancer. *Cell* 171, 1611–1624. doi:10.1016/j.cell.2017.10.044
- Putney, J. W., Jr. (1986). A Model for Receptor-Regulated Calcium Entry. *Cell. Calcium* 7, 1–12. doi:10.1016/0143-4160(86)90026-6
- Rahman, S., and Rahman, T. (2017). Unveiling Some FDA-Approved Drugs as Inhibitors of the Store-Operated Ca<sup>2+</sup> Entry Pathway. *Sci. Rep.* 7, 12881. doi:10.1038/s41598-017-13343-x
- Rathner, P., Fahrner, M., Cerofolini, L., Grabmayr, H., Horvath, F., Krobath, H., et al. (2021). Interhelical Interactions within the STIM1 CC1 Domain Modulate CRAC Channel Activation. *Nat. Chem. Biol.* 17, 196–204. doi:10.1038/s41589-020-00672-8
- Raudvere, U., Kolberg, L., Kuzmin, I., Arak, T., Adler, P., Peterson, H., et al. (2019). g:Profiler: a Web Server for Functional Enrichment Analysis and Conversions of Gene Lists (2019 Update). *Nucleic Acids Res* 47, W191–w198. doi:10.1093/nar/gkz369
- Rikova, K., Guo, A., Zeng, Q., Possemato, A., Yu, J., Haack, H., et al. (2007). Global Survey of Phosphotyrosine Signaling Identifies Oncogenic Kinases in Lung Cancer. *Cell* 131, 1190–1203. doi:10.1016/j.cell.2007.11.025
- Scrideli, C. A., Carlotti, C. G., Jr., Okamoto, O. K., Andrade, V. S., Cortez, M. A. A., Motta, F. J. N., et al. (2008). Gene Expression Profile Analysis of Primary Glioblastomas and Non-neoplastic Brain Tissue: Identification of Potential Target Genes by Oligonucleotide Microarray and Real-Time Quantitative PCR. *J. Neurooncol* 88, 281–291. doi:10.1007/s11060-008-9579-4
- Singh, A. K., Roy, N. K., Bordoloi, D., Padmavathi, G., Banik, K., Khwairakpam, A. D., et al. (2020). Orai-1 and Orai-2 Regulate Oral Cancer Cell Migration and Colonisation by Suppressing Akt/mTOR/NF-Kb Signalling. *Life Sci.* 261, 118372. doi:10.1016/j.lfs.2020.118372
- Stanta, G., and Bonin, S. (2018). Overview on Clinical Relevance of Intra-tumor Heterogeneity. *Front. Med.* 5, 85. doi:10.3389/fmed.2018.00085
- Sung, H., Ferlay, J., Siegel, R. L., Laversanne, M., Soerjomataram, L., Jemal, A., et al. (2021). Global Cancer Statistics 2020: GLOBOCAN Estimates of Incidence and Mortality Worldwide for 36 Cancers in 185 Countries. *CA A Cancer J. Clin.* 71, 209–249. doi:10.3322/caac.21660
- Suzuki, M., Jeong, S.-Y., Karbowski, M., Youle, R. J., and Tjandra, N. (2003). The Solution Structure of Human Mitochondria Fission Protein Fis1 Reveals a Novel TPR-like Helix Bundle. *J. Mol. Biol.* 334, 445–458. doi:10.1016/j.jmb.2003.09.064
- Szklarczyk, D., Gable, A. L., Lyon, D., Junge, A., Wyder, S., Huerta-Cepas, J., et al. (2019). STRING V11: Protein-Protein Association Networks with Increased Coverage, Supporting Functional Discovery in Genome-wide Experimental Datasets. *Nucleic Acids Res* 47, D607–d613. doi:10.1093/nar/gky1131
- Szklarczyk, D., Gable, A. L., Nastou, K. C., Lyon, D., Kirsch, R., Pyysalo, S., et al. (2021). The STRING Database in 2021: Customizable Protein-Protein Networks, and Functional Characterization of User-Uploaded Gene/measurement Sets. *Nucleic Acids Res* 49, D605–d612. doi:10.1093/nar/gkaa1074
- Uhlén, M., Fagerberg, L., Hallström, B. M., Lindskog, C., Oksvold, P., Mardinoglu, A., et al. (2015). Proteomics. Tissue-Based Map of the Human Proteome. *Science* 347, 1260419. doi:10.1126/science.1260419
- Vajda, S., Yueh, C., Beglov, D., Bohnuud, T., Mottarella, S. E., Xia, B., et al. (2017). New Additions to the C Lus P Ro Server Motivated by CAPRI. *Proteins* 85, 435–444. doi:10.1002/prot.25219
- Van Linde, M. E., Labots, M., Brahm, C. G., Hovinga, K. E., De Witt Hamer, P. C., Honeywell, R. J., et al. (2022). Tumor Drug Concentration and Phosphoproteomic Profiles after Two Weeks of Treatment with Sunitinib in Patients with Newly-Diagnosed Glioblastoma. *Clin. Cancer Res* 28, 1595–1602. doi:10.1158/1078-0432.ccr-21-1933

- Vangone, A., and Bonvin, A. M. (2015). Contacts-based Prediction of Binding Affinity in Protein-Protein Complexes. *Elife* 4, e07454. doi:10.7554/eLife.07454
- Vangone, A., Schaarschmidt, J., Koukos, P., Geng, C., Citro, N., Trellet, M. E., et al. (2019). Large-scale Prediction of Binding Affinity in Protein-Small Ligand Complexes: the PRODIGY-LIG Web Server. *Bioinformatics* 35, 1585–1587. doi:10.1093/bioinformatics/bty816
- Villalobos, C., Gutiérrez, L. G., Hernández-Morales, M., Del Bosque, D., and Núñez, L. (2018). Mitochondrial Control of Store-Operated Ca(2+) Channels in Cancer: Pharmacological Implications. *Pharmacol. Res.* 135, 136–143. doi:10.1016/j.phrs.2018.08.001
- Villalobos, C., Hernández-Morales, M., Gutiérrez, L. G., and Núñez, L. (2019). TRPC1 and ORAI1 Channels in Colon Cancer. *Cell. Calcium* 81, 59–66. doi:10.1016/j.ceca.2019.06.003
- Wang, J.-Y., Chen, B.-K., Wang, Y.-S., Tsai, Y.-T., Chen, W.-C., Chang, W.-C., et al. (2012). Involvement of Store-Operated Calcium Signaling in EGF-Mediated COX-2 Gene Activation in Cancer Cells. *Cell. Signal.* 24, 162–169. doi:10.1016/j.cellsig.2011.08.017
- Wang, J., Zhao, H., Zheng, L., Zhou, Y., Wu, L., Xu, Y., et al. (2021). FGF19/SOCE/NFATc2 Signaling Circuit Facilitates the Self-Renewal of Liver Cancer Stem Cells. *Theranostics* 11, 5045–5060. doi:10.7150/thno.56369
- Wang, Y.-Y., Wang, W.-C., Su, C.-W., Hsu, C.-W., Yuan, S.-S., and Chen, Y.-K. (2022). Expression of Orail and STIM1 in Human Oral Squamous Cell Carcinogenesis. *J. Dent. Sci.* 17, 78–88. doi:10.1016/j.jds.2021.07.004
- Wei, T., Simko, V., Levy, M., Xie, Y., Jin, Y., and Zemla, J. (2017). Package 'corrplot'. *Statistician* 56, e24.
- Wickham, H., Chang, W., and Wickham, M. H. (2016). Package 'ggplot2'. Create Elegant Data Visualisations Using the Grammar of Graphics. Version 2, 1–189.
- Wright, D. J., Simmons, K. J., Johnson, R. M., Beech, D. J., Muench, S. P., and Bon, R. S. (2020). Human TRPC5 Structures Reveal Interaction of a Xanthine-Based TRPC1/4/5 Inhibitor with a Conserved Lipid Binding Site. *Commun. Biol.* 3, 704. doi:10.1038/s42003-020-01437-8
- Wu, T., Hu, E., Xu, S., Chen, M., Guo, P., Dai, Z., et al. (2021). clusterProfiler 4.0: A Universal Enrichment Tool for Interpreting Omics Data. *Innovation (N Y)* 2, 100141. doi:10.1016/j.xinn.2021.100141
- Xue, L. C., Rodrigues, J. P., Kastiris, P. L., Bonvin, A. M., and Vangone, A. (2016). PRODIGY: a Web Server for Predicting the Binding Affinity of Protein-Protein Complexes. *Bioinformatics* 32, 3676–3678. doi:10.1093/bioinformatics/btw514
- Yang, S., and Huang, X.-Y. (2005). Ca2+ Influx through L-type Ca2+ Channels Controls the Trailing Tail Contraction in Growth Factor-Induced Fibroblast Cell Migration. *J. Biol. Chem.* 280, 27130–27137. doi:10.1074/jbc.m501625200
- Yang, S., Zhang, J. J., and Huang, X.-Y. (2009). Orail and STIM1 Are Critical for Breast Tumor Cell Migration and Metastasis. *Cancer Cell.* 15, 124–134. doi:10.1016/j.ccr.2008.12.019
- Yedida, G., Milani, M., Cohen, G. M., and Varadarajan, S. (2019). Apogossypol-mediated Reorganisation of the Endoplasmic Reticulum Antagonises Mitochondrial Fission and Apoptosis. *Cell. Death Dis.* 10, 521. doi:10.1038/s41419-019-1759-y
- Yu, C., Zhao, J., Yan, L., Qi, Y., Guo, X., Lou, Z., et al. (2020). Structural Insights into G Domain Dimerization and Pathogenic Mutation of OPA1. *J. Cell. Biol.* 219, e201907098. doi:10.1083/jcb.201907098
- Yu, G., Wang, L.-G., Han, Y., and He, Q.-Y. (2012). clusterProfiler: an R Package for Comparing Biological Themes Among Gene Clusters. *OMICS A J. Integr. Biol.* 16, 284–287. doi:10.1089/omi.2011.0118
- Yu, M., Nguyen, N. D., Huang, Y., Lin, D., Fujimoto, T. N., Molkentine, J. M., et al. (2019). Mitochondrial Fusion Exploits a Therapeutic Vulnerability of Pancreatic Cancer. *JCI Insight* 5, e126915. doi:10.1172/jci.insight.126915
- Zhang, J., Wei, J., Kanada, M., Yan, L., Zhang, Z., Watanabe, H., et al. (2013). Inhibition of Store-Operated Ca2+ Entry Suppresses EGF-Induced Migration and Eliminates Extravasation from Vasculature in Nasopharyngeal Carcinoma Cell. *Cancer Lett.* 336, 390–397. doi:10.1016/j.canlet.2013.03.026
- Zhang, M., Li, Q., Yu, D., Yao, B., Guo, W., Xie, Y., et al. (2019). GeNeCK: a Web Server for Gene Network Construction and Visualization. *BMC Bioinforma.* 20, 12. doi:10.1186/s12859-018-2560-0
- Zhang, Z., Xu, Q., Song, C., Mi, B., Zhang, H., Kang, H., et al. (2020). Serum- and Glucocorticoid-Inducible Kinase 1 Is Essential for Osteoclastogenesis and Promotes Breast Cancer Bone Metastasis. *Mol. Cancer Ther.* 19, 650–660. doi:10.1158/1535-7163.mct-18-0783
- Zheng, L., Stathopoulos, P. B., Schindl, R., Li, G.-Y., Romanin, C., and Ikura, M. (2011). Auto-inhibitory Role of the EF-SAM Domain of STIM Proteins in Store-Operated Calcium Entry. *Proc. Natl. Acad. Sci. U.S.A.* 108, 1337–1342. doi:10.1073/pnas.1015125108

**Conflict of Interest:** The authors declare that the research was conducted in the absence of any commercial or financial relationships that could be construed as a potential conflict of interest.

**Publisher's Note:** All claims expressed in this article are solely those of the authors and do not necessarily represent those of their affiliated organizations, or those of the publisher, the editors and the reviewers. Any product that may be evaluated in this article, or claim that may be made by its manufacturer, is not guaranteed or endorsed by the publisher.

Copyright © 2022 Hegde, Daimary, Jose, Sajeev, Chinnathambi, Alharbi, Shakibaei and Kunnumakkara. This is an open-access article distributed under the terms of the Creative Commons Attribution License (CC BY). The use, distribution or reproduction in other forums is permitted, provided the original author(s) and the copyright owner(s) are credited and that the original publication in this journal is cited, in accordance with accepted academic practice. No use, distribution or reproduction is permitted which does not comply with these terms.